



Stockamp, J., Bishop, P., Li, Z., Petrie, E. J., Hansom, J. and Rennie, A. (2016) State-of-the-art in studies of glacial isostatic adjustment for the British Isles: a literature review. *Earth and Environmental Science Transactions of the Royal Society of Edinburgh*, 106(3), pp. 145-170.

There may be differences between this version and the published version. You are advised to consult the publisher's version if you wish to cite from it.

<http://eprints.gla.ac.uk/130679/>

Deposited on: 6 November 2017

Enlighten – Research publications by members of the University of Glasgow_
<http://eprints.gla.ac.uk>

State-of-the-art in studies of glacial isostatic adjustment for the British Isles: a literature review

Julia Stockamp¹, Paul Bishop¹, Zhenhong Li², Elizabeth J Petrie¹, Jim Hansom¹ and Alistair Rennie³

¹School of Geographical and Earth Sciences, University of Glasgow, Glasgow G12 8QQ, UK.

Email: J.Stockamp.1@research.gla.ac.uk; Paul.Bishop.3@glasgow.ac.uk;
Elizabeth.Petrie@glasgow.ac.uk; Jim.Hansom@glasgow.ac.uk

²COMET, School of Civil Engineering and Geosciences, Newcastle University, Newcastle upon Tyne NE1 7RU, UK.

Email: Zhenhong.Li@newcastle.ac.uk

³Scottish Natural Heritage, Leachkin Road, Inverness IV3 8NW, UK.

Email: Alistair.Rennie@snh.gov.uk

Running heads: LH: JULIA STOCKAMP *ET AL.*

RH: STATE-OF-THE-ART OF GIA RESEARCH IN GREAT BRITAIN

1 ABSTRACT: Understanding the effects of glacial isostatic adjustment (GIA) of the British
2 Isles is essential for the assessment of past and future sea-level trends. GIA has been
3 extensively examined in the literature, employing different research methods and
4 observational data types. Geological evidence from palaeo-shorelines and undisturbed
5 sedimentary deposits has been used to reconstruct long-term relative sea-level change since
6 the Last Glacial Maximum. This information derived from sea-level index points has been
7 employed to inform empirical isobase models of the uplift in Scotland using trend surface and
8 Gaussian trend surface analysis, as well as to calibrate more theory-driven GIA models that
9 rely on Earth mantle rheology and ice sheet history. Furthermore, current short-term rates of
10 GIA-induced crustal motion during the past few decades have been measured using different
11 geodetic techniques, mainly continuous GPS (CGPS) and absolute gravimetry (AG). AG-
12 measurements are generally employed to increase the accuracy of the CGPS estimates.
13 Synthetic Aperture Radar Interferometry looks promising as a relatively new technique to
14 measure crustal uplift in the northern parts of Great Britain, where the GIA-induced vertical
15 land deformation has its highest rate. This literature review provides an in-depth comparison
16 and discussion of the development of these different research approaches.

17
18 KEYWORDS: Absolute gravity, continuous GPS, GIA modelling, mantle rheology,
19 postglacial rebound, relative sea-level change, SAR interferometry, Scotland

20
21 Glacial isostatic adjustment (GIA) is a major mechanism responsible for crustal motion of the
22 British Isles, mainly acting in a vertical direction. GIA is the visco-elastic reaction of the
23 solid Earth to the glaciation and deglaciation of its surface. During the growth of a large
24 continental ice sheet the Earth's crust and mantle are displaced downwards and sideways,
25 while the melting of an ice sheet and subsequent weight loss causes a reflux of the mantle and

1 a mainly upward motion of the crust (postglacial rebound). This continues until a state of
2 isostatic equilibrium is reached, which can be thousands of years after the deloading process.
3 Aside from vertical land motion (VLM) of the Earth's crust, the redistribution of mass of
4 surface ice, ocean water and mantle material also causes changes to the gravitational field of
5 the Earth (Fleming *et al.* 1998). Both aspects have a direct influence on relative sea-level
6 (RSL) trends at the coast, which makes analysing and understanding the dynamics of GIA a
7 critical task. The British GIA process, the effects of which are still prominent today, is mostly
8 influenced by the disappearance of the Pleistocene British-Irish ice sheet, and to a lesser
9 extent by deglaciation effects of the Laurentide and Fennoscandian ice sheets (Hansen *et al.*
10 2012). The last deglaciation of major global ice sheets began after the Last Glacial Maximum
11 (~22 kyr BP) (Shakun & Carlson 2010) and lasted well into the early Holocene (~7 kyr BP)
12 (Milne *et al.* 2006). Crustal uplift and relative land-/sea-level changes in the British Isles
13 occur with considerable spatial and temporal variability, reflecting the influences of the
14 different former ice sheets. Both the postglacial rebound of the crust, as well as the eustatic
15 sea-level changes associated with meltwater influx were comparable in magnitude (Shennan
16 *et al.* 2002). When analysing vertical land motions, several other factors also have to be taken
17 into account. These include smaller local tectonic movements, far-field effects of, for
18 example, Alpine crustal motion and flexural effects including shelf loading associated with
19 eustatic sea-level fluctuations. Further processes are continental erosion, subsidence due to
20 sediment compaction or water, gas and oil pumping, and deep mining operations, which took
21 place until the 1980s in the UK (Soudarin *et al.* 1999; Teferle *et al.* 2009). In terms of sea-
22 level changes, there are also local effects, such as tide regime changes and/or sedimentation
23 processes along the coast (Shennan *et al.* 2009).

24 Many different methods for inferring vertical land motions and/or relative land- and
25 sea-level changes, incorporating different observational data types, have been employed to

1 obtain information for constraining model parameters in GIA modelling. These methods
2 encompass the analysis of GIA through *geological reconstructions* of Late Pleistocene and
3 Holocene relative sea-level changes (e.g. Peltier & Andrews 1976; Clark *et al.* 1978;
4 Tushingham & Peltier 1991) and through modern *geodetic techniques*, such as determining
5 changes in the gravity field (e.g. Mitrovica & Peltier 1989) or three-dimensional crustal
6 motions measured by Very-Long-Baseline-Interferometry (VLBI) and GPS (e.g. James &
7 Lambert 1993; Mitrovica *et al.* 1993; Milne *et al.* 2001; MacMillan & Boy 2004). Both types
8 of field observations – geological and geodetic – have been used to inform GIA models.
9 However, there is a significant difference in the observational time scale between these two
10 data sets. The geological information describes the long-term development of GIA/RSL since
11 the Last Glacial Maximum (LGM). Modern geodetic observations, on the other hand, give
12 direct and accurate measurements of short-term or present-day GIA for the past few decades
13 only. Geodetic data can help constrain GIA models, but the long-term nature of the
14 postglacial rebound process means that modelling heavily relies on Late Devensian and
15 Holocene long-term data for calibration and parameterization of ice history and mantle
16 rheology. The short-term geodetic time-series data generally cannot fully explain those long-
17 term trends or any periodic signals in the vertical land motion. For instance, the current VLM
18 estimates (past 1–2 decades) and the long-term geologically derived VLM rates differ in 0.7
19 to -1.3 mm yr⁻¹, with the uplift in Scotland and the subsidence in South-West England being
20 lower in the geodetic short-term results (BIGF 2014).

21 This paper is an introductory overview of the different existing analytical methods of
22 observing relative sea-/land-level change and GIA-induced vertical land motion and it
23 summarizes different modelling approaches to glacial isostatic adjustment for the British
24 Isles. The suitability of relatively new methods for measuring VLM, such as SAR
25 Interferometry (InSAR), is also explored. The approach in this paper is mainly chronological,

1 but distinguishes the two principal methodologies of using (i) long-term Late Devensian/
2 Holocene geological (sea-level) data and (ii) present-day geodetic measurements for GIA
3 quantification (in sections 2 and 3, respectively).

4 In this paper, Section 1 introduces necessary terminology and reference systems for
5 the discussion of different research techniques. Section 2 focuses on using past relative sea-
6 level changes to analyse GIA, with Section 2.1 giving a short introduction to the publications
7 responsible for an extensive high-quality sea-level change data set derived from geological
8 information from various palaeo-environments between the LGM and the present (e.g.
9 Sissons 1962, 1963, 1966, 1972, 1983; Sissons *et al.* 1966; Smith *et al.* 1980, 1992, 1999,
10 2000, 2002, 2003a, 2006, 2007, 2010, 2012; Firth 1984; Firth *et al.* 1995; Cullingford *et al.*
11 1991; Shennan 1987, 1999; Shennan & Horton 2002; Shennan *et al.* 1983, 1993, 1994,
12 1995a, 1995b, 2005, 2006b). Section 2.2 discusses specifically the development and
13 refinement of empirical and theory-driven GIA models and the constraining of their
14 parameters, using these geological data (e.g. Lambeck 1993a, 1993b, 1995; Lambeck *et al.*
15 1996; Shennan *et al.* 2000, 2002, 2006a; Peltier 1998a). Section 2.3 compares published
16 maps of relative sea- and land-level changes based on the application of geological
17 information (e.g. Shennan & Horton 2002; Shennan *et al.* 2009, 2012; Smith *et al.* 2006,
18 2012).

19 Section 3 gives an insight into the literature that focuses on using geodetic techniques
20 to analyse British Isles GIA. Such geodetic studies have used continuous GPS (CGPS) and
21 absolute gravity (AG) measurements to determine crustal motions of the British Isles (Section
22 3.1) (e.g. Teferle *et al.* 2002, 2006, 2008, 2009), and those measurements have been used to
23 improve the parameterization of GIA models (Section 3.2) (e.g. Milne *et al.* 2006; Bradley *et al.*
24 2009, 2011). Section 3.3 discusses the possibilities of using InSAR for measuring crustal
25 motion in mainland Scotland, where the signal of vertical land uplift is predominant.

1. Definition of terms and reference systems

The fact that the measuring and modelling techniques explored in this paper rely on various vertical reference systems has to be kept in mind when comparing the vertical land motion or relative sea level change output of these different methods (see Fig. 1 for schematic representation). The following represents a description of these reference systems as well as a summary of the most commonly used terminology. Most cited literature in this paper can be understood against this background, though it is important to note that different meanings have emerged over the years for specific technical terms. Thus, when comparing methods and results between papers caution is required, especially if they have been written with a different perspective from either a geological, geodetic or GIA modelling field of research. Shennan et al. (2012) discusses the ambiguity of terminology in sea-level research in more detail.

In regard to the reconstruction of past relative sea level change, height measurements of sea-level index points are initially taken relative to Ordnance Datum Newlyn (ODN), for example by levelling to local benchmarks (Sissons 1962, 1963; Sissons et al. 1966; Shennan 1982). ODN is defined after local mean sea level (MSL) that was observed between 1915 and 1921 at the tide gauge in Newlyn, Cornwall and is closely approximated by a local geoid model that deviates from the global Geoid by about 80 cm. Heights above MSL in Great Britain usually relate to this vertical datum (Ordnance Survey 2015).

MSL is more generally defined as the arithmetic mean of hourly elevation measurements at a certain location for a specific period (≥ 19 years) (Woodroffe & Barlow 2015). After the geodetic definition, MSL is not a level surface and it does not exactly follow the Geoid, which is an equipotential surface. This is due to ocean dynamic effects, such as tidal forcing, ocean currents, atmospheric processes and changes in ocean density, which cause sea surface

topography. MSL and the Geoid lie close together, but can deviate from each other by a few decimetres even after averaging for tidal effects (Woodroffe & Barlow 2015).

It should be noted here that Shennan *et al.* (2012) emphasise the differentiation between the terms ‘relative land- and sea-level change’ and ‘vertical land motion’. Trying to find a common terminological ground for the GIA community, they describe sea level as the distance between the Geoid (G) (see Fig. 1), which is defined as the global time-averaged sea surface over several decades, and the solid Earth surface (R) (see also Mitrovica & Milne 2003). ‘Relative’ change always involves a change in elevation between the Geoid and the solid Earth surface, but also a change between a point in the past relative to the present day. R and G are relative to the centre of the Earth. Relative sea-level change is the negative of relative land-level change. Vertical land motion in contrast refers only to the change in elevation of the solid surface of the Earth relative to its centre. The difference between VLM and relative land-level change account for approximately -0.1 to -0.3 mm yr^{-1} around the British Isles and $+2.5$ to -1.5 mm yr^{-1} globally (Shennan *et al.* 2012, Shennan 2015). Vertical land motion combined with eustatic sea-level change results in the relative land-/sea-level change rate. If both eustatic sea level and VLM changed at the same rate in the same direction, no RSL change would be detectable.

The term ‘eustatic’ generally corresponds to changes in the volume of water in the ocean (Farrell & Clark 1976) and is used in the GIA modelling community to describe the glacio-eustatic component caused by volume changes of land surface-based ice. Any other contributions to eustasy (Fairbridge 1961) are neglected, such as a change in ocean basin geometry (tectono-eustasy) and changes in density due to variability in the heat and salinity budget of the oceans (steric effects) (Milne & Mitrovica 2008; Bradley *et al.* 2011; Peltier 2002; Fleming *et al.* 1998).

1 In addition, sea-level index points usually refer to different reference water or tide levels,
2 thus, a standardisation of the points to present mean tide level (MTL) is necessary when
3 deriving the RSL change values (Shennan *et al.* 1995a). MTL is the average of mean high
4 and mean low water (MHW/MLW) at a location. Other levels for a semidiurnal tidal system
5 include HAT – Highest Astronomical Tide, MHWS – Mean High Water Springs, MHW –
6 Mean High Water, MHWN – Mean High Water Neaps, MLWN – Mean Low Water Neaps,
7 MLW – Mean Low Water, MLWS – Mean Low Water Springs, LAT – Lowest Astronomical
8 Tide or Chart Datum (for a description see Woodroffe & Barlow 2015). Isobase models of
9 RSL change rely on height measurements relative to ODN and are then adjusted to heights
10 above MHWS, the average spring tide high water level measured over a certain period (Smith
11 *et al.* 2012; Woodroffe & Barlow 2015). Continuous GPS measurements of VLM are mostly
12 relative to a global network of points with known coordinates, the International Terrestrial
13 Reference Frame (ITRF) or regional subsets thereof, which in turn depend on its origin at the
14 long-term mean of the Centre of Mass of the total Earth System (CM) (Altamimi *et al.* 2011).
15 Absolute gravimetry (AG) also takes gravity - and subsequently height - measurements
16 relative to the Earth System's Centre of Mass. GIA models often use the Centre of Mass of
17 the solid Earth (CE) as a reference, which deviates slightly from the CM (Collilieux &
18 Altamimi 2013).

19 Furthermore, the term 'vertical land motion' represents a combination of all vertical
20 deformation effects in an area, not only GIA-induced vertical crustal motion. Strictly
21 speaking, direct geodetic measurement techniques, such as continuous GPS or InSAR, can
22 only be used to acquire information about the net vertical glacial rebound process when all
23 other vertical deformation effects can be neglected. However, the crustal uplift caused by
24 GIA can be seen as the dominant process of VLM of the British Isles over a long-term period,

so that the geodetic methods can be used as a good indicator of GIA (Bradley *et al.* 2009; Hansen *et al.* 2012).

2. Geological evidence and GIA modelling

Geological sea-level research is based on the fact that a change of sea-level influences stratigraphical successions at the coast. Deposits provide information about freshwater, marine or terrestrial sedimentation processes. Observations derived from chronological, morphological, stratigraphical and palaeontological analyses at transition zones between marine and terrestrial sediments in different locations along the coast allow reconstruction of relative sea-level changes during the Holocene. These analyses are undertaken on, ideally unconsolidated, organic and minerogenic sediments and morphological features that are related to palaeo-sea-levels and have been undisturbed by erosion or transportation since their formation (Shennan *et al.* 1995a, 2006a). Records can stem from basal or freshwater peats, partly intercalated between layers of clastic sediments, and intertidal sediment deposits of silts, clays and sands from estuaries and coastal lowlands. These are found for instance in subsidence areas of England, but also the east coast of Scotland (Shennan 1992; Shennan *et al.* 1994). In uplift areas, emerged coastal features such as raised rock platforms and beaches, gravel ridges (Fig. 2) or isolation basins (Fig. 3) play an important role. Tidal marshes, coastal wetlands and dune systems have also been analysed (Shennan *et al.* 2005). A problem is that sediments are often spatially and temporally discontinuous due to disruption by land surface processes and climate change so that a comparison of different sites becomes difficult. A common classification method in RSL reconstruction defines sea-level index points. Important groundwork for establishing sea-level curves from sea-level index points has been laid by Tooley (1974b, 1978, 1982a, b) and van de Plassche (1982), followed by a methodological approach from Shennan (1983, 1986a, b; Shennan *et al.* 1983, 1995a) that

allows the correlation of sea-level index points in different geological and geomorphological palaeo-environments on spatial and temporal scales. This happens by defining a set of characteristics, namely age, location and altitude, indicative meaning and tendency of sea-level movement. Age is determined by radiocarbon (^{14}C) dating the organic samples, supported by microfossil (pollen and diatom) analyses (Shennan 1982). Altitude is initially measured above ODN by levelling. Time and altitude are generally not enough to give unambiguous clues about sea-level falls and rises, which is why other characteristics have to be determined in order to establish relative sea-level movements. A chronology of sea-level tendencies gives information about direction of movement of sea-level (Tooley 1978; van de Plassche 1982; Shennan 1982, 1983; Shennan *et al.* 1983). This allows separation of transgression and regression overlaps in the sediments, indicated by vegetation and/or lithology changes. This includes the alternation of terrestrial or freshwater sediments with marine sediments due to eustatic sea-level changes, land uplift or subsidence and changes in sedimentation rate and deposited material (Tooley 1982b). The indicative meaning places a sample's location in relation to a contemporary reference tide level so that comparisons between various sampling areas are made possible. Depending on the type of deposited material this can refer to Mean High Water of Spring tides (MHWS), Mean Tide Level (MTL) or Highest Astronomical Tide (HAT) (Shennan 1992; Shennan *et al.* 1995b) (see also Fig. 1). Additionally, an indicative range states information about the accuracy of the indicative meaning. Finally, in order to determine rates of RSL change, a linear trend is fitted to the age–sea-level height plots of observations (Shennan 1989; Shennan & Horton 2002).

2.1. Building up a data bank of Late Devensian and Holocene sea-level observations

Since the late 20th century several studies have been undertaken to collect data on Late Devensian and Holocene relative sea-level change from palaeo-environments in Great

1 Britain, thus accumulating a rich data bank of sea-level index points that help constrain GIA
2 model parameters and reduce existing model discrepancies (e.g. Tooley 1974b; Shennan
3 1989; Shennan *et al.* 1995a, 2000, 2005, 2006b; Shennan & Horton 2002). Extending the
4 comprehensive analysis by Shennan (1989) of all then-available radiocarbon data on sea-
5 level index points, Shennan *et al.* (1995a) summarized the information gained from various
6 studies undertaken in north-western Scotland (between Kentra Bay and Loch Morar)
7 (Shennan *et al.* 1993, 1994, 1995b). Previous studies had focused predominantly on eastern,
8 northeastern and southern Scotland (Sissons *et al.* 1966) or the east coast of England
9 (Shennan 1992), where sedimentary environments for sea-level research are available in
10 abundance. Few stratigraphic studies had been undertaken in western Scotland prior to
11 Shennan *et al.*'s studies, due to the lack of appropriate depositional or sedimentary
12 environments in that region, except for the south-western part of Scotland (e.g. Jardine,
13 1980). The rest of Great Britain, in contrast, exhibits more wide-ranging estuarine deposits
14 that can be used for GIA studies. Shennan *et al.* (1995a) thereby established a broad data set
15 of Late Devensian and Holocene relative sea-level changes from 12 kyr ^{14}C BP to the present,
16 the main elements of which are a rapid fall of sea-level of about 9 mm/ ^{14}C yr before 10 kyr
17 ^{14}C BP, followed by an almost stationary sea-level in the early Holocene, which was
18 succeeded by a rise of sea-level to a mid-Holocene highstand with a subsequent fall in the
19 Late Holocene (Shennan *et al.* 2000).

20 Shennan *et al.* (2005) added new sea-level index point observations to that database
21 from isolation basins, raised tidal marshes, coastal wetlands and dune systems located around
22 Arisaig, northwestern Scotland. They created a 16,000-year record of relative sea-level
23 changes from the time of deglaciation after the Last Glacial Maximum to the present. In
24 particular, they presented new data on the mid-Holocene RSL highstand (reached between

1 ~7,600-7,400 cal yr BP and 6.74 ± 0.2 m above present) and on the Laurentide and Antarctic
2 ice sheet duration.

3 Other studies within a second school of thought of RSL research have also
4 contributed substantially to the observational information about Holocene RSL change. These
5 focused on collecting direct altitude measurements along prominent palaeo-shorelines in
6 sheltered inlets and estuaries, and provided chronological information from stratigraphical
7 analyses, instead of chronological and altitudinal analyses in isolation basins. The shoreline
8 data have been used to model isobase maps of the pattern of uplift in Scotland (see also
9 section 2.3).

10 Raised shorelines, caused by glacio-isostatic uplift, are basically marine limits at
11 inland margins that are characterised by distinctive features in their morphology and
12 stratigraphy (Smith *et al.* 2000). The temporal sequence of raised shorelines during the
13 Holocene enables the reconstruction of Holocene uplift patterns. Early investigations on
14 visible and buried raised beaches, with shoreline altitudinal measurements and detailed
15 morphological analyses in Scotland were conducted by Sissons (1962, 1963, 1966, 1969),
16 Sissons *et al.* (1966), Smith (1968), Smith *et al.* (1978), Kemp (1976), Dawson (1979, 1980,
17 1984) and Firth & Haggart (1989). The work of Sissons and co-workers (e.g. Sissons 1962,
18 1963; Sissons *et al.* 1966) provided an important re-definition of raised shorelines and their
19 heights, with focus on southeastern Scotland, by pioneering the application of levelling
20 techniques based on OD benchmarks.

21 Among the four main and most visible shorelines is the Storegga Slide Tsunami
22 Shoreline, which has been analysed, for example, by Smith *et al.* (2000, 2004, 2006, 2012)
23 and Dawson *et al.* (2011). The shoreline reached immediately before the tsunami struck along
24 the east coast of Scotland in the mid Holocene, is dated at around 8,100 cal yr BP (Dawson *et al.*
25 *et al.* 2011). Smith *et al.* (2000) used altitude observations, along with stratigraphic and

1 microfossil analysis of sediments at the inner margin of the estuarine surface at the time of
2 the tsunami, thus enabling the modelling of uplift of mainland Scotland since the tsunami.
3 Deposition of tsunami sediments was rapid and essentially synchronous at each coastal
4 location, thereby avoiding diachroneity that often compromises the determination of the uplift
5 pattern in glacial rebound areas (Smith *et al.* 2004).

6 Altitudinal data have also been collected from the Main Postglacial Shoreline and
7 analysed by Sissons *et al.* (1966), Sissons (1972, 1983), Smith (1968), Smith *et al.* (1980,
8 1992, 1999, 2000, 2002, 2003a, b, 2006, 2007, 2010, 2012), Firth (1984), Firth *et al.* (1995),
9 Cullingford *et al.* (1991), Selby & Smith (2007), Jordan *et al.* (2010), and Dawson (1984),
10 among others. This shoreline is dated at 6,400-7,700 cal yr BP when the Main Postglacial
11 Transgression occurred (Mcintyre & Howe 2010). It was for a long time believed to be the
12 highest shoreline, but the Blairdrummond Shoreline, modelled by Smith *et al.* (2000, 2006,
13 2007, 2012), overlaps with the Main Postglacial Shoreline at the margin of glacio-isostatic
14 uplift (Smith *et al.* 2007, 2012). The Blairdrummond Shoreline has been dated at 4,500-5,800
15 cal yr BP (Mcintyre & Howe 2010). Smith *et al.* (2006, 2012) also mention the Wigtown
16 Shoreline, which is visible in a terrace below the Blairdrummond Shoreline and dated at
17 1,520–3,700 cal yr BP (Mcintyre & Howe 2010). A note on the empirical modelling
18 approaches based on this shoreline data, compared to the more theory-driven, rheological
19 GIA models, is given in the following section.

20 21 **2.2. GIA modelling approaches constrained by Late Devensian and Holocene RSL** 22 **data**

23 These kinds of high-quality and long-term sea-level reconstructions around the British Isles
24 have been used for model calibration and validation in a range of studies developing high-
25 resolution glacio-isostatic rebound models of the British Isles (e.g. Lambeck 1993a, b, 1995;

Lambeck *et al.* 1996; Shennan *et al.* 2000, 2002, 2006a; Peltier *et al.* 2002; Milne *et al.* 2006).

GIA models usually encompass (1) an Earth-model for the isostatic signal that is related to the solid Earth deformation due to surface mass redistribution between ice sheets and oceans; (2) a model of the ice sheet evolution during the Late Pleistocene; and (3) a (sea-level change) model for the re-distribution of ocean water resulting from ice mass changes, incorporating the sea-level equation (Milne *et al.* 2006; Shennan *et al.* 2006a). Earth-models in GIA modelling usually contain several layers of varying densities, elastic parameters and viscosities, for which various values can be found in the literature (see Fig. 4). These layers include a lithosphere with a certain thickness, one or more upper-mantle layers with different viscosities – alternatively a more detailed depth-dependent viscosity structure – and a lower mantle viscosity below the 670 km seismic discontinuity. The Earth-model is usually described by a spherically symmetric, self-gravitating Maxwell body (Bradley *et al.* 2011).

For the ice model, parameters such as ice sheet dimensions and thickness and the temporal evolution of ice build-up and melting are significant over the entire Late Pleistocene/ Holocene period, since the effects of (melt-)water loading and the ice-equivalent eustatic contribution on the RSL observations (including any major meltwater pulses) have a major influence on model output.

The UK sea-level dataset provides important constraints on GIA model parameters, such as lithospheric thickness, upper mantle viscosity, near-field ice sheet history of the British Isles, global/far-field deglaciation history and magnitude and rate of global meltwater discharge (Shennan *et al.* 2005). However, the modelling studies also show that observations are difficult to fit with a single ice-Earth model combination and no unique solution has been found for the explanation of relative sea-level observations, one reason being the sensitivity of the GIA process to both near- and far-field effects (Milne *et al.* 2006). Great Britain's

1 proximity to Fenno-Scandinavia and the large mass of the former Fennoscandian ice sheet
2 mean that RSL and glacial rebound are not only influenced by the former British-Irish ice
3 sheet. Additional contributions by loading–unloading of the crust due to the Fennoscandian
4 ice sheet, its meltwater and gravitational attraction of the ocean water, have to be taken into
5 account in Scottish GIA modelling (Lambeck 1991). Present-day uplift in Fennoscandia can
6 reach up to 10 mm yr^{-1} , calculated for example from long-term tide gauge records and
7 corrected with a eustatic sea-level rise of 1.2 mm yr^{-1} (Steffen & Wu 2011). Absolute gravity
8 and continuous GPS measurements show the same rate, with an uplift centre in the northern
9 Gulf of Bothania (Johansson *et al.* 2002; Steffen & Wu 2011).

10 Lambeck (1993a, b) provided the first comprehensive modelling studies of British
11 sea-level evidence and discussed parameterization of the Earth-model and ice-model that
12 determines the sea-level predictions. Both papers developed a forward-modelling-inverse-
13 modelling process that allows determination of the optimum ice sheet (ice thickness and ice
14 sheet margins) and Earth rheology parameters for Great Britain for the Late Pleistocene and
15 Holocene from the then-existing geological sea-level data. Lambeck (1993a) formulated the
16 requirements for simulating the glacial rebound with a high precision and resolution of better
17 than 1m, such as inclusion of the Fennoscandian ice sheet for far-field effects, consideration
18 of different ice sheet load cycles and the Loch Lomond Readvance. Including sea-level
19 observations from inside and outside of the glacial margins allowed separation of Earth-
20 model parameters from ice sheet parameters in the inversion of the GIA equations. Starting
21 with a simple first- and second-order rebound model in Lambeck (1993a), the author
22 eventually presents a more complex GIA model (Lambeck 1993b). This includes a more
23 detailed ice-model for the Late Devensian ice sheet for the period between maximum
24 glaciation and the end of the Loch Lomond Readvance. New estimates of mantle viscosity
25 were presented, concluding that the mantle is mostly homogeneous from the base of the

lithosphere to the 670 km boundary. Optimum mantle parameter values were given for lithospheric thickness (65 km), mantle viscosity above 670 km ($\sim 4\text{--}5 \times 10^{20}$ Pa s) and below 670 km ($> 4 \times 10^{21}$ Pa s) (see Fig. 4). Apart from the uncertainties in the ice sheet over northern Scotland (Beaully Firth area) and Ireland, the observations were generally well fitted. In an additional study, Lambeck (1995) examined what further information can be derived about coastal shoreline evolution from the GIA model. He investigated the derivation of British Isles palaeo-bathymetry and palaeo-shorelines from glacio-isostatic rebound models and established, for instance, the maximum emergence of the North Sea with relative sea-level stagnation after the start of deglaciation from about 15,000 to 12,000 radiocarbon years BP, allowing shoreline features to be formed along eastern Scotland's long and shallow marine inlets (firths). After around 10,000 yr BP, a rapid retreat of shorelines could be modelled.

A general GIA modelling problem is that a broad range of possible parameter combinations in the Earth-model lead to similar predictions and equally good fits to the observations, with no unique determination of the parameters possible (Lambeck & Johnston 1998; Bradley *et al.* 2009). Another in the series of Lambeck papers (Lambeck *et al.* 1996) further examined this trade-off between lithospheric thickness and upper-mantle viscosity. A thin lithosphere leads to low upper-mantle viscosity, whereas a thick lithosphere causes a high viscosity with similar modelling results, and the solutions might not represent the optimum in the model parameter space anyway but only local minima. Thus, Lambeck *et al.* (1996) explored a broad range of parameter values in a model that incorporates one lithosphere layer and up to four mantle layers with each having a different viscosity. The effective values that lead to the optimum solution in the parameter space for this revised five-layer model are stated in their paper (see also Fig. 4).

While Lambeck's modelling achieved good fit between model results and observations, discrepancies remained in the model of the British ice sheet, particularly in northern Scotland with an underestimation of rebound. Therefore, more detailed geological observations were necessary for constraining parameters for the Late Devensian ice sheet. Shennan *et al.* (2000) thus added new data to the previously limited and isolated data points in northwestern Scotland, helping to constrain glacio-hydro-isostatic rebound model parameters. The authors examined the validation of models that simulate relative sea-level change using a revised version of Lambeck's (1993a, b) model. They summarized the observational radiocarbon data from data index points since Late Devensian deglaciation to the present, from raised tidal marshes and isolation basins in northwest Scotland (Kentra, Arisaig, Kintail, Applecross, Coigach). The best overall agreement was achieved with only three mantle layers in the Earth-model with a lithospheric thickness of 65 km, an upper mantle viscosity of 4×10^{20} Pa ^{14}C s and a lower mantle viscosity of 10^{22} Pa ^{14}C s, based on values determined by Lambeck *et al.* (1998) (see Fig. 4). A sensitivity analysis showed that the Earth-model was more sensitive to lithospheric thickness than to upper- or lower-mantle viscosity; however, the Earth-model was not the primary source for high discrepancies. Rather, the British ice sheet model had larger uncertainties. In contrast to the previous optimum ice-model (Lambeck 1993b, 1995), the ice thickness had to be increased by 10 % north of the Great Glen to account for the discrepancies between predictions and observations in that area (Lambeck 1993b). But despite that improvement, the model of the British ice sheet still showed inadequacies and a re-examination of various combinations of Earth- and ice-model again highlighted the non-uniqueness and parameter trade-off problem within the model (Shennan *et al.* 2000).

In contrast to Lambeck (1993a, b) and Shennan *et al.* (2000), a second broad modelling strategy by Peltier *et al.* (2002) and Shennan *et al.* (2002) approached the GIA

1 problem in a more global sense, including far-field RSL data. Peltier *et al.* (2002) attempted
2 the validation of the ICE-4G (VM2) global model of glacial rebound containing a revised
3 viscosity model (VM2) originally derived from global GIA observations (e.g. Peltier, 1974,
4 1994, 1996a, b, 1998a, b; Peltier & Jiang 1996). There are two inputs for the model: a global
5 model of the deglaciation history since the LGM and a model that describes the radial
6 variation of the viscosity from the Earth's surface to the boundary between mantle and core.
7 The authors included considerations of effects from global deglaciation of far-field ice sheets,
8 such as Laurentia and Antarctica, on RSL change of Scotland and its viscoelastic structure
9 near the surface. They found that lithospheric thickness, to which the rebound model is most
10 sensitive, had to be reduced from 120 km to 90 km to achieve better model fits. This was
11 based on a proposed constraint by Ballantyne (1997), Ballantyne *et al.* (1998) and McCarroll
12 & Ballantyne (2000) on the maximum thickness of the LGM ice sheet over Scotland, which
13 lead to a reduction of the maximum of the LGM Scottish ice sheet thickness from about 2200
14 m to 1200 m. Peltier *et al.* (2002) argued that Lambeck's lower mantle viscosity in the order
15 of 10^{22} Pa s does not fit relaxation times in other GIA regions, like Canada, where a value up
16 to 2×10^{21} Pa s is more appropriate. In addition, considering a low sensitivity to the much
17 smaller ice load of the British-Irish ice sheet, the viscosity value should be even lower for the
18 British Isles. They also varied the lower mantle viscosity with depth with an increase to $5 \times$
19 10^{21} Pa s at 1300 km (see Fig. 4).

20 Shennan *et al.* (2002) further examined Peltier *et al.*'s (2002) ICE-4G (VM2) global
21 model and concentrated on remaining discrepancies between model predictions and
22 observations in Great Britain, focusing on a revised local British Isles ice-model and also on a
23 validation of global models of the far-field ice melt history in Antarctica fitting the RSL
24 change around the British Isles.

Apart from differences in mantle viscosity values, the Peltier *et al.* (2002) and Shennan *et al.* (2002) GIA model (henceforth denoted by Model B) varies from the Lambeck (1995) and Shennan *et al.* (2000) model (Model A) in many aspects. Some of the differences between the two implementations can be summarized as follows. There are different radial viscoelastic structures (three-layer Earth model in Model A versus a smoother viscosity gradient throughout the mantle in Model B) and a significant difference in lithospheric thickness (65 km in Model A versus 90 km in Model B). This is mainly due to the methodological approaches of Peltier *et al.* (2002) and Shennan *et al.* (2002) including global teleconnections in the deglaciation process and far-field data to validate GIA models. They differ in the pattern of meltwater eustatic sea-level change and inclusion of global meltwater events, and use different time scales. Model A applies a radiocarbon time-scale in line with the geological observations, Model B, however, applies a calendar year time-scale, with Peltier *et al.* (2002) arguing that the ^{14}C time-scale introduces biases in the interpretation of the GIA observations and the estimation of Earth model parameters.

Both GIA model implementations also use different British Isles ice sheet models, but both utilize the UK geological data to constrain ice dimensions. Both generally show a good degree of fit, but no unique solution for observations from all locations (Shennan *et al.* 2006a). Those differences are explained in more detail by Shennan *et al.* (2006a), who used the previous findings to create a revised GIA model for the British Isles and Ireland ice sheets, with the British and Scandinavian ice sheets converging over the North Sea, contrary to previous beliefs. They also consider an underlying terrain correction underneath the ice sheet, which had not been applied before, and which is especially important in high terrain regions, such as the Scottish Highlands as shown by Fretwell *et al.* (2008).

Further work has been done recently for the British Isles in regard to numerical modelling of the dynamic evolution of the British-Irish ice sheet. Instead of relying only on

ice sheet history, i.e. extent and thickness of the ice sheet informed by geomorphological data, the output of physically-based ice flow models was used as input for the up-to-date GIA models in an attempt to increase their accuracy (Kuchar *et al.* 2012).

It is important to note that over the years contrasting concepts of RSL/GIA studies and modelling approaches have emerged for investigating the spatial distribution of uplift based on observational Late Devensian and Holocene sea-level data. Aside from the GIA modelling studies discussed above, other RSL analyses have been undertaken, using empirical shoreline-based models to describe the spatial pattern of RSL change. A comparison of both approaches can be found in Smith *et al.* (2006, 2012) and Shennan *et al.* (1995a). The theory-driven GIA models use estimates of ice/water loading and unloading, Earth mantle rheology and sea surface change for the estimation of RSL, while the empirical shoreline-based models use trend surface analyses or polynomial regression of shoreline altitudes of relict shore features (Smith *et al.* 1969). An early trend surface model was developed by Cullingford *et al.* (1991), discussing the altitude and age variation of the Main Postglacial Shoreline in eastern Scotland. Other studies dealing with this approach are those of Firth *et al.* (1993), Smith *et al.* (2000, 2006, 2012) or Fretwell *et al.* (2004). Firth & Haggart (1989) reconstructed the pattern of isostatic uplift by drawing isobases perpendicular to the declination of the analysed palaeo-shorelines.

These shoreline-based models also often rely on a different understanding of the temporal evolution of Holocene RSL. Tooley (1974a, 1982b), Smith (2005) and Smith *et al.* (2012) identified oscillating behaviour in the Holocene RSL change, while GIA models assume non-oscillating Holocene RSL trends. Smith *et al.* (2012), for instance, investigated the temporal and spatial pattern of RSL change in northern Britain and Ireland with a shoreline-based modelling approach developed by Smith *et al.* (2006) using a Gaussian Trend Surface Model. That model was fitted to the shoreline altitude data from four decades of RSL

1 studies. The altitude measurements were taken at the inner margins of Holocene estuarine
2 terraces supported by morphological, stratigraphic, microfossil and radiocarbon analyses.
3 Smith *et al.* (2012) found evidence for four main episodes from the Younger Dryas to the late
4 Holocene, in each of which RSL is first rising to a culminating shoreline and then falling
5 again. Metre-scale fluctuations were identified without the smooth gradually changing curves
6 that theory-driven GIA models rely on and indeed predict. They also mapped the newest
7 altitude data and spatial pattern/isobases of the Storegga, Main Postglacial, Blairdrummond
8 and Wigtown shorelines. The spatial pattern of RSL change in Smith *et al.* (2012) reflect the
9 general glacio-isostatic uplift pattern, with an elliptical form and a trend of decreasing
10 altitude towards the margin of the uplift zone (compare Figs 5 and 6 in the following section).

11 Noteworthy is also a range of studies investigating the relation between glacio-
12 isostatic uplift and neotectonic activity during the Late Devensian and Holocene in Scotland.
13 They indicate that the temporal and spatial uplift pattern in isostatic recovery areas of
14 Scotland may be more complex due to neotectonic effects than the simple pattern of isobase
15 maps derived from shoreline data or geophysical models would imply (Firth & Stewart
16 2000). Early investigations found evidence that former shorelines in glacial-isostatic uplift
17 areas may not have been uniformly uplifted. The uplifted shorelines rather exhibit a distorted
18 form: horizontal or gently sloping blocks of crust separated by sharp jumps in altitude. This
19 variation in shoreline gradients has been described by Sissons (1972) in the Western Forth
20 Valley, complemented by another study in the Glen Roy region (Sissons & Cornish 1982;
21 Sissons, in press). The differential movement of blocks can be seen as a minor form of crustal
22 movements compared to the major long-term glacio-isostatic uplift. They are either related to
23 an immediate reaction to glacier loading/unloading of the Loch Lomond Readvance as in the
24 Forth area, or to lake level changes as in the Glen Roy region. The crustal dislocations in both
25 places happened along faults and relate to former earthquake activity during isostatic rebound

(Sissons & Cornish 1982). The idea of localised dislocation of isostatically uplifted shorelines mostly caused by fault movement during the Late Devensian and Holocene is also supported by a range of other studies of neotectonic activity in other parts of Scotland (Gray 1974, 1978; Firth 1984, 1986, 1992; Ringrose 1987, 1989; Smith et al. 2009).

Some earlier studies differ in the magnitude and cause of crustal displacements, linking glacial rebound to high seismic activity in the Holocene (e.g. Davenport and Ringrose 1985, Davenport et al. 1989, Ringrose et al. 1991) with 10^1 - 10^2 m of lateral motion along faults due to large magnitude postglacial earthquakes. Opposing that view are Firth & Stewart (2000) and Stewart et al. (2001), arguing for a rather low seismotectonic activity with only metre-scale vertical movements along pre-existing fault lines. Firth & Stewart (2000) summarize the investigations of vertical shoreline displacements that happened along fault lines during uplift in mainland Scotland. Most of the shoreline dislocations or jumps coincide with (pre-existing) faults and zones of crustal weakness, on a scale of mainly between 1 and 2.7 m during the Late Devensian and Holocene. Across Scotland those displacements often but not exclusively occurred in the vicinity of the Younger Dryas Stadial ice margin, indicating that not only tectonic but also glacio-isostatic rebound stresses in the crust associated with ice loading and deloading explain seismotectonics in the Scottish Highlands.

2.3. Maps of Holocene relative sea- and land-level changes

The extensive observational data base of Holocene sea-level index points and the different GIA modelling efforts have led to various reconstructions of long-term relative land- and sea-level changes. Figure 5a shows an early map by Shennan (1989), which identifies the centre of uplift in western central Scotland with up to 2.0 mm yr^{-1} , corresponding to the area of maximum ice thickness at the LGM, and a maximum subsidence of -2.0 mm yr^{-1} in southeast England. In comparison, Shennan & Horton (2002) show a more detailed map, due to a

greater amount of available sea-level evidence. They used 1200 radiocarbon dates constraining RSL change in Great Britain over the past 16,000 years to calculate net rates of late Holocene land-level and sea-level changes. Figure 5b shows highest relative land uplift (equal to relative sea-level fall, but with opposite sign) in western and central Scotland with ca. 1.6 mm yr⁻¹. Maximum subsidence occurs in southwest England with ca. 1.2 mm yr⁻¹. The subsidence rates in the south and east of England in the 1989 map are higher, since a correction for sediment consolidation is missing.

Shennan *et al.* (2012) provided a revised map of late Holocene relative land- and sea-level rates, based on the recent GIA modelling advances (Shennan *et al.* 2006a; Brooks *et al.* 2008; Bradley *et al.* 2011) constrained by geological sea-level indicators. Figure 5c displays the centre of relative uplift again over central Scotland due to GIA; however, the areas of relative subsidence are more differentiated with three sub-centres over southwest England, the southern North Sea and the Shetland Isles, demonstrating other governing factors, including ocean loading as well as far-field GIA signals. Furthermore, in contrast to 2002 the value of the relative uplift of Scotland is again lower in the 2012 results, with correspondingly reduced rates of relative subsidence in England. Those differences can be explained by an increase in observational data, improvement of the models, and further consideration of sediment compaction (Shennan *et al.* 2009, 2012).

In comparison, the results within the second school of thought of Holocene RSL research (Smith *et al.* 2006, 2012) show a similar spatial pattern of relative sea-level changes, based on shoreline altitude measurements and Gaussian Quadratic Trend Surface isobase modelling. The prominent shorelines in Figure 6 are a result of relative stability of vertical land motion and RSL changes. The Main Postglacial Shoreline emerges as the highest one in the uplift centre of Scotland with 10 m relative to Mean High Water Ordinary Spring Tides (MHWS). The Blairdrummond Shoreline is the second highest shoreline, with 8 m MHWS,

1 followed by the Wigtown Shoreline with 6 m MHWS, which is the youngest and lies on top
2 of other shorelines at the margins of Scotland. The Storegga Shoreline is located below the
3 other shorelines, with 4 m MHWS at its maximum altitude (Smith *et al.* 2012).

4 5 **3. Geodetic measurement techniques and GIA modelling**

6 Geodetic measurements provide a second broad type of data to quantify crustal motion and
7 hence potentially to constrain GIA model parameters or to correct sea-level trends at tide
8 gauges. These geodetic measurements are of present (vertical) crustal motion over monthly,
9 annual and perhaps decadal timescales, and their relationship to, and consistency with, the
10 quantification of GIA using geological information on sea-level change has yet to be fully
11 assessed.

12 Geodesy is a powerful tool for monitoring crustal motions worldwide; however,
13 detecting vertical movement often presents more of a challenge due to its magnitude of about
14 1-10 mm yr⁻¹, compared to horizontal tectonic movement of about 1-15 cm yr⁻¹ (Soudarin *et*
15 *al.* 1999). Space-based, airborne or ground-based methods, such as Very Long Baseline
16 Interferometry (VLBI), measurements of the gravity field, Global Navigation Satellite
17 Systems (GNSS), Satellite Laser Ranging (SLR) or Doppler Orbitography and
18 Radiopositioning Integrated by Satellite (DORIS) and a combination thereof have shown
19 potential to produce (direct) estimates of present-day vertical land motion (VLM) and thereby
20 to quantify GIA rates (e.g. Ashkenazi *et al.* 1993; James & Lambert 1993; Mitrovica *et al.*
21 1993; Peltier 1995; Argus 1996; Argus *et al.* 1999; Larson & van Dam 2000; Lambert *et al.*
22 2001; Hill *et al.* 2010).

23 Regarding northern Britain, the DORIS, SLR and VLBI techniques suffer from
24 limitations in vertical resolution, since their networks are too sparse and their stations too far
25 away from the centre of postglacial rebound in Scotland to be sensitive to the GIA signal.

Thus, for the British Isles, the main geodetic techniques applied for measuring VLM are absolute gravimetry (AG) and continuous GPS (CGPS). Those estimates are often used for the correction of tide gauge records to derive climate induced sea-level change by removing the vertical land motion component from the relative sea-level trends.

3.1. Point measurements of crustal motions

3.1.1. Absolute gravimetry. Gravity measurements have been used in the past to quantify various geodynamic processes that have influence on the gravitational field on different spatial and temporal scales, from ocean tides and groundwater changes to sea-level changes, plate boundary deformation and long-term postglacial rebound (Lambert *et al.* 2006). Gravimetry is a valuable geodetic observation tool that contributes to the precise definition of a common Geoid, a global reference system and explanation of geodynamic processes. Gravitational field measurements can be taken both from space (e.g. Gravity Recovery and Climate Experiment – GRACE; or ESA’s Gravity Field and Steady-State Ocean Circulation Explorer - GOCE) and in terrestrial approaches (e.g. stationary absolute gravimeters) for mass redistributions in, for example, the mantle of the Earth in response to glacial rebound. As well as for the British Isles, those measurements have been applied in several other glacial rebound areas, such as Laurentia (Lambert *et al.* 2001; Tamisiea *et al.* 2007) and Fennoscandia (Hill *et al.* 2010).

For the UK, Williams *et al.* (2001) presented some preliminary results for the absolute gravity technique for three tide gauges for a 3–4-year measurement period beginning in Newlyn and Aberdeen in 1995 and in Lerwick in 1996. Gravity is measured by dropping a test mass, a corner-cube retroreflector, in a vacuum. This happens every 10 s, while measurements by an iodine stabilized He–Ne laser interferometer together with a rubidium atomic clock allow the equations of motion for acceleration of the mass to be solved

(Niebauer *et al.* 1995; Williams *et al.* 2001; Teferle *et al.* 2007). Measurements are taken, for instance, every year for 3–4 days at each site. The sites are located on stable bedrock, and regular intercomparisons with other gravimeters in Europe and the USA allow a consistently good accuracy within 1–2 μGal to be maintained (Williams *et al.* 2001). Today’s accuracy of gravity measurements is about 10^{-9} g (1 μGal or 10nm/s^2), which translate to height changes of about 3 mm relative to the Earth centre of mass (Forsberg *et al.* 2005; Blewitt *et al.* 2010). Different ratios between gravity change rates and vertical displacement rates for conversion of gravity values to vertical land motion can be found in the literature, but Williams *et al.* (2001) assume a change in gravity of 0.2 μGal is associated with a height change of 1 mm. Results show vertical land motion of 1.0 ± 1.4 mm yr^{-1} at Newlyn, southwest England, -3.8 ± 1.6 mm yr^{-1} at Lerwick, Shetland, and 0.9 ± 3.1 mm yr^{-1} at Aberdeen, Scotland, mostly reflecting the general glacio-isostatic pattern in the UK.

3.1.2. Continuous GNSS. The use of Global Navigation Satellite Systems (GNSS), especially Global Positioning System (GPS), is widely applied for direct measurements of surface displacement and vertical crustal motions of the British Isles. The technique of continuous GPS measurements is frequently used near tide gauge stations to derive the vertical station velocities from height coordinate time-series. A high precision of more than 1 mm yr^{-1} can be achieved with this technique using a few years of observations (Blewitt *et al.* 2010). The advantages of using GPS at tide gauges were recognized as early as 1990 with episodic GPS in the UK following recommendations of Carter *et al.* (1989). Subsequently, several campaigns were implemented by the Institute of Engineering Surveying and Space Geodesy (IESSG) and the Proudman Oceanographic Laboratory (POL) (Bingley *et al.* 2001). Early studies on determining GPS station heights in the UK and testing their accuracy were undertaken, for example, by Ashkenazi *et al.* (1993). The importance of permanent measurements in the form of continuous GPS (CGPS) at tide gauges was

emphasised in 1993 by the International Association for Physical Sciences of the Ocean (IAPSO) Committee (Carter 1994). The number of CGPS stations worldwide has increased rapidly since 1993, in conjunction with increasingly cheaper GPS receivers and better computer hardware and software, with the main purpose to realize the International Terrestrial Reference System (the newest one being the ITRF2008, with ITRF2014 under preparation). In the UK, the establishment of CGPS stations at tide gauges by IESSG and POL for the measurement of VLM commenced in 1997 (Teferle *et al.* 2006). Today, around 160 operating CGPS stations can be found UK-wide, according to the UK Ordnance Survey. The application of CGPS in conjunction with absolute gravity measurements has been implemented by IESSG and POL since the late 1990s in the UK, with the establishment of three AG stations in the proximity of tide gauges (Teferle *et al.* 2007).

Permanent GPS observations have also been extensively used in Fennoscandia, mostly in large-scale campaigns within the BIFROST (Baseline Inferences for Fennoscandian Rebound Observations, Sea-Level and Tectonics) project (Johansson *et al.* 2002; Milne *et al.* 2001, 2004; Lidberg *et al.* 2007). GPS benefits from the fact that receivers are based on the ground and not on the satellite. Thus, the receivers can be used more flexibly at different locations. GPS equipment has also become increasingly cheaper and with a range of scientific-quality software packages available the processing of GPS observations is more accessible. CGPS stations can be set up directly at tide gauge locations, thus being representative of the VLM at this station excluding other deformation effects from surrounding areas. The direct link with the International Terrestrial Reference Frame (ITRF) theoretically allows tide gauge benchmarks to be connected via a common global reference frame and thus making comparisons of sea-level datasets possible (Wöppelmann *et al.* 2006). However, it has to be considered that several external and internal GPS error sources can introduce biases in station time-series and velocities, especially in the vertical component,

leading to increased scatter and higher uncertainty compared to the horizontal components.

Creating false signals in the GPS estimates, such error sources are for example:

- Variations in the phase centres of satellite and receiver antennas;
- Ionospheric and tropospheric delays and mismodelling thereof in the processing;
- Atmosphere, ocean and surface hydrologic loading;
- Uncertainties in satellite orbits;
- Multipath due to reflection from surrounding objects;
- Satellite and receiver clock errors;
- Unaccounted geophysical processes;
- Unfavourable satellite constellation leading to dilution of precision;
- Realisation or constraints of the reference frame applied.

For geophysical analysis, GPS observation periods should be at least 2.5 years in length to allow estimation of annual and semi-annual signals and obtain realistic velocity estimates (Blewitt & Lavallée 2002).

For the UK, Bingley *et al.* (2001) presented some preliminary results from episodic GPS (EGPS) campaigns between 1991 and 1996 combined with the first five continuous GPS stations (Sheerness, Newlyn, Aberdeen, Liverpool and Lowestoft) and gave a first impression of the magnitude of VLM at tide gauges, which corresponds to results derived from long term relative sea-level observations in Woodworth *et al.* (1999) in the range of 0–3 mm yr⁻¹. Sanli & Blewitt (2001) analysed the tide gauge North Shields in Northeast England in terms of VLM, derived from a single GPS campaign directly tied to the tide gauge benchmark. They evaluated GPS as an alternative method to the use of GIA models for the correction of sea-level trends and confirmed its capability to derive independent estimates of sea-level change. The VLM at the station accounted for 0.6 ± 1.5 mm yr⁻¹, with an associated geocentric sea-

level rise of 2.6 ± 1.0 mm yr⁻¹. Considering that the tide gauge measurement alone (1.8 mm yr⁻¹) would have underestimated geocentric sea-level rise, they emphasised the importance of correcting tide gauge records for postglacial rebound.

Concentrating on refining GPS methodology, Teferle *et al.* (2002) tested the method of using dual-continuous GPS stations for monitoring vertical land motion at tide gauges, which involves one GPS directly at the tide gauge, that measures the actual VLM of this station, and another one within a range of a few kilometres on stable bedrock that allows separating short-term motions of the tide gauge structure itself from underlying geophysical processes. This concept for long-term station velocity monitoring had already been mentioned by Bingley *et al.* (2001) and was originally proposed by Plag *et al.* (2000). With the dual-CGPS concept, Teferle *et al.* (2002) addressed the known issue of biases in coordinate time-series caused by temporal or spatial correlations. Their approach facilitates the removal of those systematic effects, which are common to both time-series, by differencing the coordinate time-series of both stations and thus obtaining a coordinate time-series with fewer systematic biases.

3.1.3. Continuous GPS combined with absolute gravimetry. The common biases that result in loss of accuracy and precision in CGPS can be addressed by using spatial filtering techniques that effectively limit parameter uncertainty (e.g. Wdowinski *et al.* 1997; Johansson *et al.* 2002; Dong *et al.* 2006). Among the possible reasons for the systematic biases in GPS estimates named above are errors in the International Terrestrial Reference Frame (ITRF), which influence vertical station velocity (Altamimi *et al.* 2007, 2011). The accuracy of CGPS depends heavily on the accuracy of the ITRF and difficulties remain in determining the geocentre of the ITRF and its motion relative to the Earth's centre of mass (Blewitt 2003; Dong *et al.* 2003; Teferle *et al.* 2007, 2009).

Absolute gravity (AG) measurements of VLM, however, show good accuracy in general, since those kinds of biases are missing here. AG is independent of the International Terrestrial Reference Frame (Teferle *et al.* 2009). Thus, AG measurements can help assess CGPS estimates of vertical land motion. The issue with the accuracy of CGPS measurements (systematic offsets from other observation techniques) has been dealt with by Teferle *et al.* (2006, 2007), for instance, by aligning the CGPS estimates with AG measurements. For nine tide gauges in the UK and northern France, the authors demonstrated, how the integration of the two techniques can contribute to more reliable estimates of the vertical station velocities using time-series starting in 1997 for CGPS and 1995/6 for AG. They compared alternatives to their CGPS/AG method for deriving vertical land motion, including (1) using geological evidence; (2) the inverse of the difference between the mean sea-level trend at British tide gauges and an assumed absolute sea-level rise of 1.5 mm yr^{-1} for northern Europe (see also Woodworth *et al.* 1999); and (3) using GIA models. They pointed out a systematic offset between CGPS estimates on the one hand and the AG estimates as well as those other independent estimates of VLM on the other hand. Other authors have also found a systematic offset between CGPS and the outputs of AG, GIA models and Very Long Baseline Interferometry measurements for stations in Europe and North America, with CGPS generally being more positive. The causes lie within the GPS processing chain (antenna phase centre modelling, reference frame realisation etc.) (Teferle *et al.* 2009).

The AG-alignment encompasses a calculation of the offset between the CGPS and AG-based VLM estimates, which account for $1.2 \pm 0.4 \text{ mm yr}^{-1}$ (Teferle *et al.* 2007), and which is consistent with the offset between CGPS and other independent techniques, as well as values found in the literature (MacMillan 2004; Prawirodirdjo & Bock 2004). In a next step, the weighted mean difference between the vertical station velocity estimates from CGPS and AG is calculated and afterwards subtracted from the CGPS estimates, which results in the

1 AG-aligned CGPS estimates of vertical crustal motions (Hansen *et al.* 2012). Results of those
2 estimates of vertical station velocity in Teferle *et al.* (2007) lead to a de-coupled absolute sea-
3 level rise of about $1.3 \pm 0.3 \text{ mm yr}^{-1}$ around the British Isles. But due to remaining
4 uncertainties in the CGPS and AG time-series the statistical significance of these results
5 could not be established yet.

6 Teferle *et al.* (2009) extended this survey and compared the results of different
7 independent CGPS processing strategies, including the effects of spatial filtering and
8 reference frame implementations for deriving CGPS and AG-aligned CGPS estimates of
9 present-day vertical as well as horizontal crustal motion. Their two processing strategies
10 involved (1) a daily double-difference (DD) regional network (RN) solution, produced from
11 1997 to 2005 (DDRN) and (2) a series of daily precise point positioning (PPP) globally
12 transformed (GT) solutions from 2000 to 2005 (PPPGT). In the first approach a regional
13 reference frame with four European IGS (International GNSS Service) stations within the
14 ITRF2000 was implemented. The second processing strategy used a globally extended
15 reference frame with the 99 IGS stations within the IGS realisation of the ITRF2000.
16 Additionally, they compared filtered and unfiltered results with regard to spatial correlation
17 in the time-series. For validation purposes, they used derivations of vertical crustal motion
18 based on the Holocene geological information on relative sea-level trends from Shennan &
19 Horton (2002) and Shennan *et al.* (2006b). The authors concluded that a simultaneous
20 processing using two or more independent CGPS processing solutions is important to get the
21 best possible or most realistic results from station data. They showed that geodetic techniques
22 complement each other and that an independent data set for validation, such as geological
23 information, is crucial.

24 Figure 7 shows their results and differences between CGPS only (Fig. 7a, b) and AG-
25 aligned CGPS (Fig. 7c, d) estimates of vertical station velocity for Great Britain for the two

CGPS processing solutions DDRNF and PPPGTF. Those geodetic results of present-day crustal motions confirm the general trend of the geological map of Holocene data (see Fig. 5), which is subsidence in the area of Shetland and in most of England and Wales, and uplift in most areas of Scotland. Offsets in vertical station velocities between DDRNU and PPPGTU account for $1.1 \pm 1.1 \text{ mm yr}^{-1}$, and $0.7 \pm 0.6 \text{ mm yr}^{-1}$ between DDRNF and PPPGTF (regional vs. global reference frame realisation). Those offsets between processing strategies could again be significantly reduced with AG-alignment. The systematic offsets between AG and CGPS are stated as 1.5 and 1.3 mm yr^{-1} for DDRNU and DDRNF respectively relative to AG and 0.6 mm yr^{-1} for both PPPGTU and PPPGTF relative to AG, with the CGPS estimates being more positive in all cases. As the maps show, the geodetic results vary significantly between each other in spatial distribution and magnitude of the vertical land motion shown, depending on what CGPS processing strategy (with regional or global reference frame implementations) has been used or whether AG-alignment has been performed.

Hansen *et al.* (2012) presented an update on present-day vertical land motion in the UK from CGPS and AG-aligned CGPS measurements. In contrast to the results of Teferle *et al.* (2009), stations in Northern Ireland are included, which allows defining the western boundary of uplift due to GIA in the north of the UK (see Fig. 8b, compared to Fig. 7). A re-processing of the BIGF (British Isles continuous GNSS Facility) network (daily-double differenced solutions within a semi-global reference frame realisation, ITRF2005, of 37 IGS stations) for the period between 1997 and 2008 involved a re-assessment of the stations that are representative of crustal motion, by analysing surface and bedrock geological data, site photographs and monumentation data, and an exclusion of stations with time-series lengths of less than six years. For Scotland, where continuous measurement periods were mostly shorter than that, the dual-CGPS approach (Teferle *et al.* 2002) was applied. Thus, 46 stations across the UK were determined as appropriate for geophysical research (Hansen *et al.* 2012).

Additional to the maps from 2005 (Teferle *et al.* 2009) and from 2008 (Hansen *et al.* 2012) other AG-aligned CGPS maps of current vertical crustal uplift have been published, a few of which are presented in Figure 8. Generally, more and more stations have been included over the years, since the observation period per station has become longer and many new stations now fulfil the minimal time-frame requirement. When comparing the maps, the different reference frame implementations and subsets or regional realisations thereof (ITRF2000, ITRF2005, ITRF2008, IGB08 etc.) have to be kept in mind, as they are likely to cause offsets between the maps. A shift of the uplift centre's location within Scotland is noticeable. It cannot be clearly defined and depends on the applied processing strategy or the amount of total stations included, among other factors. In Teferle *et al.* (2009) the maximum uplift tends towards the East for the PPPGTF solution, with $1.6 \pm 0.3 \text{ mm yr}^{-1}$ in Edinburgh. In Bradley *et al.* (2009) (Figure 8a) it is visibly located in eastern Scotland with $1.07 \pm 0.35 \text{ mm yr}^{-1}$ in Edinburgh. The processing of this data considered motion relative to the station in Sheerness in southeast England. Hansen *et al.* (2012) included data from Ireland and the uplift centre shifts towards western Scotland, similarly to the BIGF map from 2010 (Fig. 8b, c). This is more consistent with GIA model outputs. The BIGF map from 2015 (Fig. 8d) places it again more towards central/eastern Scotland, and shows a spatially more diverse pattern with the increasing number of stations included. For example, highest values can be found in DRUM with $1.43 \pm 0.36 \text{ mm yr}^{-1}$, EDIN with $1.38 \pm 0.23 \text{ mm yr}^{-1}$, KILN with $1.30 \pm 0.39 \text{ mm yr}^{-1}$ and BRAE with $1.30 \pm 0.42 \text{ mm yr}^{-1}$ (BIGF 2015).

Such geodetically derived comprehensive data sets of present-day vertical crustal motions of the British Isles provide the data basis (horizontal and vertical station velocity estimates) for further studies, including the work of Woodworth *et al.* (2009), who estimated rates of mean sea-level change around the UK from tide gauges, and that of Milne *et al.* (2006) and Bradley *et al.* (2009, 2011), who concentrated on the improvement of GIA models

using CGPS data for further parameter constraint. The latter technique is elaborated in more detail in the next section.

3.2. GIA modelling approaches with parameter constraints from CGPS

GIA modelling studies (e.g. Lambeck 1993a, b; Peltier *et al.* 2002; Shennan *et al.* 2000, 2002) produced good overall results for the pattern of general relative sea-level (RSL) change but they failed to provide good fits at all observation sites, and tended to underestimate the extremes of RSL change observations (Shennan & Horton 2002). With the emergence and refinement of the CGPS technology, several attempts at modelling glacial rebound have been undertaken that include both the geological Holocene RSL evidence and the information gained from CGPS measurements to constrain modelling parameters. With this new data source the aim is now no longer to reproduce Holocene RSL curves, but rather use the GIA models (calibrated with Holocene sea-level evidence) to predict today's short-term vertical land motion, for which CGPS observations give important clues for further parameterization.

The most obvious contribution of CGPS data to GIA modelling is that CGPS provides information from spatially more evenly distributed observation points as well as about the UK's interior, while RSL indicators were limited to the coast.

Milne *et al.* (2004) and (2006) utilized the advantage that CGPS gives information about three-dimensional crustal motions, including the horizontal velocity field induced by GIA, whereas sea-level data can only provide indirect measurements of vertical movement. They validated the present-day model predictions of horizontal crustal motion of GIA against the CGPS observations of 12 stations in the UK. The authors aimed to address the weaknesses of previous GIA models (Lambeck 1993a, b; Peltier *et al.* 2002; Shennan *et al.* 2002), such as the risk of overestimation of the ice thickness in regions with high terrain like northwest Scotland, since the earlier applied ice-models had assumed a flat topography

1 underneath the ice layer. They found that previously the ice thickness had been overestimated
2 by up to 500 m, and that now with terrain-correction the model fit could be improved. They
3 also endorsed a rather rapid ice growth phase culminating in the Last Glacial Maximum.
4 Therefore, Peltier *et al.* (2002) – assuming an equilibrium ice sheet before the LGM – had
5 overestimated vertical deformation after deglaciation. However, the study of Milne *et al.*
6 (2006) also demonstrated the emergence of new modelling difficulties while trying to achieve
7 a good fit of the GIA model to both the RSL and the CGPS data.

8 Bradley *et al.* (2009) extended Milne's *et al.* (2006) study by examining the
9 information content of the entire 3D-velocity field of the GIA component in Great Britain,
10 introducing the vertical GPS deformation information (see Fig. 8a), since the time-series were
11 now long enough to reach the required accuracy for the vertical coordinate. They tried to
12 analyse the measured and modelled vertical land motion component that is caused by the
13 British-Irish ice sheet only, thus using relative CGPS deformation values between the station
14 in Sheerness and the rest of the UK, and eliminating the influence from far-field ice sheets.
15 Figure 9 illustrates the two components of the complete modelled signal of present-day land
16 uplift (Fig. 9a) after decomposition into the signal from the non-local ice sheets (Fig. 9b) and
17 from the British-Irish ice sheet and ocean (Figure 9c). It shows the subsidence for all of the
18 British Isles caused by the Fennoscandian ice sheet with a magnitude of more than 1 mm yr⁻¹.
19 The general pattern of the total current vertical land motion signal is consistent with the
20 spatial distribution of relative motion in previous modelling results of Late Holocene RSL
21 change (see Fig. 5) with an SSW-NNE oriented ellipse of an upward trend in Scotland and
22 North Ireland with the centre in central western Scotland and subsidence in most of England.

23 Despite encountering the parameter trade-off problem again, Bradley *et al.* (2009)
24 found that the CGPS data provide a robust constraint for the upper mantle viscosity, and thus

suggested that an integration of Holocene sea-level and modern CGPS data will better constrain the viscosity structure model of the Earth.

Bradley *et al.* (2011) presented the latest study in GIA modelling for the British Isles, drawing upon a variety of constraints from several previous studies: Bradley *et al.* (2009) for the constraint of the Earth-model viscosity values from the CGPS data; Shennan *et al.* (2006a) and Brooks *et al.* (2008) for the British-Irish ice component of the model, based on an integration of geomorphological field constraints from both Great Britain and introducing Ireland; and a non-local/global ice-model combined from Bassett *et al.* (2005) and Bradley *et al.* (2008), the latter extending the melting period further into the Holocene with far-field RSL data for the prediction of eustatic sea-level change. The authors found an improvement in model fits due to a revised (lower) magnitude of the predicted Holocene highstands. Settling on a certain set of optimum Earth-model parameters, they achieved a high-quality fit to RSL and CGPS data with a lithospheric thickness of 71 km, and an upper- and lower mantle viscosity of 5×10^{20} Pa s and 3×10^{22} Pa s respectively.

Figure 10 shows maps of the present-day vertical land uplift of about 0.95 mm yr^{-1} at a maximum (Fig. 10a) and relative sea-level change for the British Isles from this revised optimum model combination with a relative fall of up to -1.1 mm yr^{-1} (Fig. 10b). Splitting the total signal into far-field ice sheet effects and the British-Irish ice sheet signal only, shows a sea-level rise from far-field ice sheets of 0.8 mm yr^{-1} across Scotland (Fig. 10c). This has a dampening effect on the relative sea-level fall associated with the British-Irish ice sheet only, which accounts for up to 1.7 mm yr^{-1} over central Scotland (Fig. 10d).

3.3. Potential of SAR Interferometry for monitoring land uplift in northern Britain

Postglacial rebound has been investigated utilising a variety of measurement and modelling methods. Another powerful space geodesy tool for doing so might be found in Synthetic

Aperture Radar (SAR) Interferometry. Differential SAR Interferometry (DInSAR) is an established technique for analysing crustal motions and land deformations in terms of co-seismic processes, landslides or volcanic activity (e.g. Wright *et al.* 2003, 2004b; Pritchard *et al.* 2006; Samsonov & d'Oreye 2012; Feng *et al.* 2014; Singleton *et al.* 2014; Remy *et al.* 2015). But it has also been widely used as a method for monitoring slower surface movements on a longer time scale, like inter-seismic deformation or land subsidence due to groundwater and oil withdrawal or mining activities. It is also often combined with CGPS observations or levelling techniques as an independent data source (e.g. Hoffmann *et al.* 2001; Tosi *et al.* 2002; Carbognin *et al.* 2004; Wang *et al.* 2008; Chen *et al.* 2010; Fan *et al.* 2011; Osmanoğlu *et al.* 2011; Aobpaet *et al.* 2013; Leighton *et al.* 2013). DInSAR has been proven useful for giving indirect information about GIA in areas where the ice sheet is still present. For example, it has been used in Antarctica to measure ice mass change and glacier flows and thus present clues about glacial rebound of the Antarctic continent (Sasgen *et al.* 2010). However, research examining the applicability of DInSAR for monitoring wide-scale GIA land uplift directly, in any GIA affected region, is relatively scarce. So the question for future research is what can be achieved at the direct interface between DInSAR and GIA (see Fig. 11).

A review of DInSAR and land deformation monitoring is given by Massonnet & Feigl (1998) and Crosetto *et al.* (2005). Recent advances using DInSAR time-series approaches for crustal deformation measurement are reviewed by Hooper *et al.* (2012). With conventional radar interferometry two complex SAR images of the same area, acquired at the same time, but from different positions (measuring topography), or at different times (measuring deformation), are combined to generate an interferogram. For this, one acquisition is multiplied by the complex conjugate of another acquisition. See Hanssen (2001) for an in-depth description of the process. The phase of the interferogram is the phase difference

1 between the two acquisitions, which is sensitive to surface height/topography and range
2 changes in the line of sight of the radar. Conventional InSAR has been mostly used for
3 generating topographic maps, prominently in the Shuttle Radar Topography Mission
4 (SRTM). Temporal land surface changes are derived with Differential Interferometry, where
5 usually a DEM is subtracted from the interferogram to eliminate the topographic phase from
6 the total phase signal in order to obtain the deformation phase component. An important
7 prerequisite is that scattering properties on the ground stay the same, in order to create a high
8 coherence between images and make the interferometric process possible. Usually, the longer
9 the radar wavelength, the better a sensor is suited for the mitigation of such decorrelation
10 effects. Data is available from several SAR platforms, such as ESA's ERS-1/ERS-2, ESA's
11 ENVISAT ASAR, ESA's recent Sentinel-1 mission, the Canadian Radarsat-1/-2, the
12 Japanese ALOS PALSAR and ALOS-2 PALSAR, the Italian Cosmo-SkyMed and from the
13 German TerraSAR-X (see Fig. 12). Together they contribute to an abundant global archive of
14 SAR images for approximately the past 20 years, in different frequency bands of X-, C- and
15 L-band and thus make it theoretically possible to observe GIA-related land uplift, for
16 example in Scotland.

17 For the detection of long-term and very small, long-wavelength displacements, such as GIA,
18 a very high quality standard in terms of precision and accuracy is necessary to make it a
19 competitive tool to established geodetic techniques, such as CGPS (Crosetto *et al.* 2005).

20 Under the right conditions, DInSAR can be sensitive to land deformations in the low
21 mm-level (Crosetto *et al.* 2005; Marinkovic *et al.* 2008). The accuracy of DInSAR time series
22 techniques lies at 1 mm yr^{-1} for mean deformation velocity (Hammond *et al.* 2012), but is
23 dependent on weather conditions, the number of acquisitions available, the total time range
24 covered by images and the distance to the reference area (Lanari *et al.* 2007; Hooper *et al.*
25 2012).

To achieve such precision and accuracy conventional DInSAR techniques, where only two images are used, are insufficient. Over the last decade, methods for detecting long-term deformation have been improved by stacking several spaceborne SAR images of the same area, acquired through time. In this way, it is possible to describe the temporal evolution of deformations. Two prominent time-series techniques are known. The first one analyses the phase behaviour and scattering characteristics of a point scatterer in time and thus identifies pixels with minimal decorrelation noise (Persistent Scatterer) (Ferretti *et al.* 2001; Hooper *et al.* 2004; Costantini *et al.* 2008). The second technique focuses on distributed scatterers and only uses interferograms between SAR images that are characterised by a small temporal and spatial baseline, so that decorrelation noise is minimised. An inversion of the interferograms then reveals the underlying cumulative deformation signal (Small Baseline Subset InSAR or SBAS) (Berardino *et al.* 2002; Lanari *et al.* 2004, 2007). In case of high data redundancy, which means that several acquisitions are available for the observed area, a good precision and robustness can be achieved addressing problems such as decorrelation and atmospheric and orbital effects (Crosetto *et al.* 2005).

In general, the accuracy of the height change is only as good as the accuracy of the interferometric phase, which is influenced by several error sources. The total phase signal in an interferogram is usually a summation of several phase components: $\phi_{total} = \phi_{deformation} + \phi_{orbit} + \phi_{atmosphere} + \phi_{topography} + \phi_{noise}$ (Hanssen 2001), all of which have to be corrected for, when trying to extract the deformation signal $\phi_{deformation}$ from ϕ_{total} .

A major limitation is finding areas with sufficient coherence of the ground targets. Temporal decorrelation or phase noise (ϕ_{noise}) is the most challenging problem with DInSAR, especially in terms of very slow land uplift (GIA) or subsidence. Very slow motion is more prone to temporal decorrelation because it requires a longer observation period. This

phenomenon can be addressed by bandpass filtering before interferogram generation, interferogram filtering or multi-looking (Hooper *et al.* 2012). The permanent monitoring of slow deformation with CGPS has an advantage here because it is not prone to such decorrelation effects. In addition, uncertainties in the DEM information that has been used for generating the differential interferogram cause topographic phase residuals ($\phi_{topography}$), which have to be considered and corrected (Ferretti *et al.* 2000; Crosetto *et al.* 2005).

Additionally, the time-series techniques noted above address limits due to artefacts, superimposing signals due to atmospheric disturbances ($\phi_{atmosphere}$) and uncertainties of satellite orbit parameters (ϕ_{orbit}). Those non-deformation artefacts can “swallow” the small motion process of GIA-induced uplift by introducing systematic errors in the DInSAR observations of displacements. Changes in atmospheric propagation between two acquisitions cause a signal delay and thus range differences. This atmospheric phase screen (APS) can become manifest in long radar wavelengths, such as L-band, caused by the ionosphere, and, more commonly, across all radar frequencies due to tropospheric disturbances. The former is more of a problem in the case of long-wavelength deformation processes over hundreds of kilometres, while the latter presents a challenge for non-linear, non-steady deformations happening on a scale of tens of kilometres (Hooper *et al.* 2012). In the case of a constant deformation rate, averaging/stacking several interferograms can decrease errors such as atmospheric effects (Hoffmann *et al.* 2001; Wright *et al.* 2001). However, estimating the non-deformation signal by modelling approaches is even better than averaging. Methods have been developed that use external information about atmospheric conditions (water vapour). The information may come from weather models, spectrometers, CGPS data about the tropospheric delay of a signal (Li *et al.* 2005, 2006, 2009, 2012) or relating topographic height with interferometric phase (Bekaert *et al.* 2015).

Orbital artefacts or phase ramps are especially problematic when it comes to measuring long-wavelength wide-scale ground deformation (GIA), since both often show similar spatial patterns, which are difficult to distinguish. Those errors are caused by inaccurate information about the orbit trajectories of the satellite at the times of acquisition. Algorithms for orbital error reduction take advantage of the fact that orbit errors are usually considered as uncorrelated over time, in contrast to deformation signals (Biggs *et al.* 2007; Zhang *et al.* 2014). They simply fit either linear planes or 2-dimensional polynomials empirically to the errors (Massonnet & Feigl 1998; Wright *et al.* 2004a), and subtract them from the interferometric phase of an individual interferogram. Quadratic functions need to be applied with images covering more than 1000 km (Fournier *et al.* 2011). However, if the deformation signal shows similar characteristics, as is to be expected in the case of GIA land uplift in northern Britain, this would eliminate the deformation signal from the interferograms as well. This means more sophisticated methods are necessary, such as utilizing networks of interferograms, rather than a single one, to fit planes to interferometric phases (Biggs *et al.* 2007). Based on this network orbit correction technique, Feng (2014) and Stockamp *et al.* (2015) applied an extended method, which combines the conventional network approach with phase loop triplets of interferograms in order to introduce further observation equations that constrain parameters better. Another alternative is to use a network of interferograms for modifying orbit state vectors and estimating baseline errors directly (Bähr & Hanssen 2010, 2012). Furthermore, the separation of the long-wavelength deformation signal from orbital artefacts with GPS measurements is possible (e.g. Argus *et al.* 2005; Pritchard *et al.* 2006; Brooks *et al.* 2007; Lundgren *et al.* 2009; Arkan *et al.* 2010; Gournelen *et al.* 2010; Wei *et al.* 2010; Manzo *et al.* 2012; Wang & Wright 2012; Béjar-Pizarro *et al.* 2013; Kaneko *et al.* 2013; Tong *et al.* 2013). The techniques to overcome problems in deformation extraction are continuously improved by the use of more frequent acquisitions, better elevation and

1 atmospheric correction models and more sophisticated methods of Precise Orbit
2 Determination for better accuracy of satellite orbits.

3 Combination with another geodetic technique, such as CGPS, is also essential, when
4 it comes to validation of the DInSAR results. In general, validation could be difficult in
5 regard to the extension of the ground areas that are covered by DInSAR, when reference
6 validation data are only sparse. The reference data must also be of equally high quality to that
7 of the DInSAR data regarding precision and accuracy (Crosetto *et al.* 2005).

8 The applicability and potential of DInSAR for determining vertical land motion
9 (VLM) in the mm-level and in the context of relative sea-level change have been
10 demonstrated by Brooks *et al.* (2007), for instance. They derived the VLM (induced by
11 groundwater and oil extraction) at the coast of the Los Angeles basin between 1992 and 2000
12 with a Persistent Scatterer InSAR approach (C-band), tide gauge and CGPS observations.
13 InSAR helped in determining the large spatial variability of VLM in that area, allowing the
14 relative sea-level in regions far away from tide gauge stations to be calculated along the coast
15 with a high spatial resolution.

16 Persistent Scatterer (PS) InSAR has also been successfully established on a regional
17 level in Great Britain as a complementary technique to GPS and absolute gravity
18 measurements for the monitoring of vertical land level changes. Its applicability has been
19 demonstrated in urbanised areas, for example in the River Thames region (Bingley *et al.*
20 2007). Adamska (2012) tested the suitability of using PS InSAR to measure regional VLM
21 around selected tide gauges in the UK (Newlyn, Sheerness, Liverpool, North Shields), and to
22 assess their stability, by referencing the relative InSAR measurements to absolute CGPS
23 estimates. The author achieved good results for PS velocities despite unwanted influences by
24 ocean tide loading on the deformation of the coastal areas.

For measuring more wide-spread glacial rebound in the UK, and especially in the central uplift regions of Scotland, the wide area coverage requires processing of bigger amounts of image data, although this could be limited by focusing on stable (exposed rocky) surfaces. SBAS could be more suitable than PS InSAR due to the rural nature of most parts of the uplift area and the scarceness of dominant scatterers, such as man-made structures. This, however, also depends on the temporal sampling rate of acquisitions. In terms of addressing the issue of coherence in rural areas, the Intermittent SBAS (ISBAS) (Sowter *et al.* 2013; Cigna *et al.* 2014b) approach, which includes intermittently or partially coherent areas, looks promising. The problem of temporal decorrelation might not be as much of a problem in northern Britain as it is in other GIA areas, such as Scandinavia or Canada. Due to its maritime climate the snow cover period is shorter and less extensive in northern Britain. In addition, the land cover is more suitable for getting a good coherence for X- and C-band radar data, due to the lack of boreal forest or other forms of higher vegetation. This means that even shorter radar wavelengths (X- and C-band) might not be as affected by decorrelation (Rosen *et al.* 1996).

In mountainous regions (highlands) DInSAR is seen as challenging. Liu *et al.* (2014), however, showed the application of SBAS for subsidence monitoring with L-, C- and X-band in a mountain area in China and produced promising results. In addition, a feasibility study undertaken by the British Geological Survey assessed the usability of PS-InSAR to monitor ground motion on a nationwide scale in Great Britain, by investigating the use of appropriate SAR geometry of ERS-1/2 and ENVISAT to counteract geometric distortions, such as foreshortening, layover and shadowing, caused by local topography (Cigna *et al.* 2012, 2013, 2014a). Overall topographic visibility was determined to be good, i.e. active layover could only be found in a small proportion of Great Britain. Layover usually occurs at slopes facing the sensor and when the slope angle is steeper than the SAR incidence angle. Then the upper

1 part of the slope is seen as equally far away from the sensor as the lower slope part and both
2 areas appear at the same location in the SAR image or are laid over each other. This can
3 happen mostly in the very hilly regions of Scotland, and is dependent on the acquisition mode
4 of ‘ascending’ or ‘descending’ and the orientation of the hill slopes towards the radar sensor’s
5 line of sight. No major shadow effects were discovered due to the reasonably flat mountain
6 slopes in Great Britain (Cigna *et al.* 2012).

7 To summarise, the continuous two-dimensional monitoring capabilities of DInSAR
8 provide the advantage of measuring the GIA-induced vertical land motion directly over large
9 areas (over 100 km wide swaths), in contrast to techniques that focus on single point
10 measurements and spatial interpolation. Many coherent points over the surface can be
11 evaluated at relatively low effort and costs, and there is no ground measurement technique
12 that could basically provide the same amount of sampling points. Thus, DInSAR could
13 account better for the spatial variability of vertical land motion and its implications for
14 relative sea-level trends, and it is not limited to the CGPS/AG/tide gauge network in Britain.

16 **4. Conclusion**

17 Several investigations that attempt to improve quantification and modelling of past and
18 present glacial isostatic adjustment of the British Isles have been conducted in the last
19 decades. This paper reviews some of those efforts in regard to the different observational data
20 types, such as geological Late Devensian/ Holocene sea-level evidence and present-day
21 geodetic information, which have been used for the constraint of GIA model parameters for
22 the British Isles. An extensive data bank of sea-level index points from palaeo-environments
23 around the British Isles has been built up that motivated the development of a variety of GIA
24 models and helped in the derivation of long-term Holocene relative sea- and land-level
25 estimates. Later studies examined the advantage of geodetic techniques, mainly CGPS, which

1 help further parameterize the GIA models and give insight specifically into present-day
2 vertical land motion. Despite this advance in GIA modelling for the British Isles, difficulties
3 in parameterization persist and poor fits between model and observations remain not
4 uncommon, especially in Scotland. Different modelling approaches have tried to fit the same
5 Holocene sea-level data, but significant differences regarding ice sheet history and Earth-
6 model parameters remain in the modelling community. These misfits reflect the complex
7 GIA situation of the British Isles with a significant spatial and temporal variability in sea- and
8 land-level change since the Last Glacial Maximum. The local isostatic component of the sea-
9 level signal is of similar magnitude to that associated with the melt-water contribution from
10 non-local ice sheets, but with opposite signs near the British ice sheet centre. Thus, strong
11 non-monotonic sea-level changes were caused in time in the UK (Lambeck 1993a, b; Milne
12 *et al.* 2006; Bradley *et al.* 2009; Rennie & Hansom 2011).

13 Maps of both the relative land-level change modelled with help of geological
14 evidence (Shennan & Horton 2002; Shennan *et al.* 2009) and the modelled vertical land
15 motion constrained by data from geodetic techniques (Bradley *et al.* 2009, 2011) show a
16 similar pattern with the centre of maximum uplift near the south-western Grampian
17 Highlands of Scotland, consistent with most CGPS maps. However, the studies have also
18 shown that geodetically derived estimates of vertical land motion can vary, depending on
19 what CGPS processing strategy, time-series analysis approach and correction for temporal
20 and spatial correlations has been used to derive the deformation velocities. In addition, the
21 offset between CGPS and AG measurements in the vertical coordinate of $\sim 1\text{mm yr}^{-1}$, as
22 reported by Teferle *et al.* (2009), cannot be ignored considering the magnitude of the
23 postglacial rebound signal is not much higher on the British Isles.

24 It is always important that results from the different geological and geodetic
25 techniques are interpreted and compared with care, since they differ in applied processing and

analysis methods, spatial sampling rates, time-scales, reference frames (relative land-/sea-level change or vertical land motion), and the consideration of non-GIA related geophysical effects that influence crustal movements and sea-levels.

Further research might give deeper insights into current rates of land uplift in northern Britain and its implications for relative sea-level change, by combining multiple satellite techniques, especially GNSS and SAR Interferometry. Although notable challenges have to be expected, when deriving very small, long-wavelength deformation signals from DInSAR data, techniques are in place to correct for these errors and limit uncertainties. The advantage of DInSAR is its high accuracy and spatial resolution, covering a wider area. It could close gaps in the quantitative description of the spatially diverse distribution of GIA, since the observational data density of conservative methods varies between regions. Geodetic methods provide information mostly limited to the existing CGPS/AG network, while Late Devensian/Holocene geological data are confined to accessible and preserved palaeo-environments. As another independent data source, DInSAR can help address biases in other geodetic techniques and vice versa, thus demonstrating a complementary relationship between geodetic methods, as shown with CGPS and AG. Therefore, DInSAR might be beneficial in answering questions like to what extent GIA-induced crustal uplift is still an issue at Scottish coasts today (Rennie & Hansom 2011) and thus, if a higher impact of rising sea-levels at coasts is to be expected after all.

5. Acknowledgements

JS is supported by an EPSRC industry scholarship in association with Scottish Natural Heritage. The work is supported in part by the UK Natural Environment Research Council (NERC) through the LICS project (NE/K010794/1), the Key Laboratory of Earth Fissures Geological Disaster, Ministry of Land and Resources (Geological Survey of Jiangsu

Province) through the KEYLAB/InSAR project as well as the JAXA ALOS RA4 project (PI: 1358).

The services of the Natural Environment Research Council (NERC) British Isles continuous GNSS Facility (BIGF), www.bigf.ac.uk, in providing archived GNSS data (and/or products) to this study, are gratefully acknowledged.

The authors thank David E. Smith and the anonymous referee for their valuable comments and their time spent on reviewing the manuscript.

6. References

Adamska, L. M. 2012. *Use of Persistent Scatterer Interferometry for the enhancement of vertical land movement measurement at tide gauges around the British coast*. Doctoral Dissertation, University of Nottingham, UK.

Altamimi, Z., Collilieux, X., Legrand, J., Garayt, B. & Boucher, C. 2007. ITRF2005: A new release of the International Terrestrial Reference Frame based on time series of station positions and Earth Orientation Parameters. *Journal of Geophysical Research: Solid Earth* (1978–2012) **112**.

Altamimi, Z., Collilieux, X. & Métivier, L. 2011. ITRF2008: an improved solution of the international terrestrial reference frame. *Journal of Geodesy* **85**, 457-473.

Aobpaet, A., Cuenca, M. C., Hooper, A. & Trisirisatayawong, I. 2013. InSAR time-series analysis of land subsidence in Bangkok, Thailand. *International Journal of Remote Sensing* **34**, 2969-2982.

Argus, D. F. 1996. Postglacial rebound from VLBI geodesy: On establishing vertical reference. *Geophysical Research Letters* **23**, 973-976.

- 1 Argus, D. F., Peltier, W. R. & Watkins, M. M. 1999. Glacial isostatic adjustment observed
2 using very long baseline interferometry and satellite laser ranging geodesy. *Journal of*
3 *Geophysical Research-Solid Earth* **104**, 29077-29093.
- 4 Argus, D. F., Heflin, M. B., Peltzer, G., Crampé, F. & Webb, F. H. 2005. Interseismic strain
5 accumulation and anthropogenic motion in metropolitan Los Angeles. *Journal of*
6 *Geophysical Research: Solid Earth (1978–2012)* **110**.
- 7 Arıkan, M., Hooper, A. & Hanssen, R. 2010. Radar time series analysis over west anatolia.
8 *Proceedings Fringe 2009 Workshop, Frascati, Italy*. European Space Agency (Special
9 Publication) ESA SP-677.
- 10 Ashkenazi, V., Bingley, R. M., Whitmore, G. M. & Baker, T. F. 1993. Monitoring changes in
11 mean-sea-level to millimeters using GPS. *Geophysical Research Letters* **20**, 1951-1954.
- 12 Bähr, H. & Hanssen, R. F. 2010. Network adjustment of orbit errors in SAR interferometry.
13 *Proceedings Fringe 2009 Workshop, Frascati, Italy*. European Space Agency (Special
14 Publication) ESA SP-677.
- 15 Bähr, H. & Hanssen, R. F. 2012. Reliable estimation of orbit errors in spaceborne SAR
16 interferometry. *Journal of Geodesy* **86**, 1147-1164.
- 17 Ballantyne, C. K. 1997. Periglacial trimlines in the Scottish Highlands. *Quaternary*
18 *International* **38**, 119-136.
- 19 Ballantyne, C. K., McCarroll, D., Nesje, A., Dahl, S. O. & Stone, J. O. 1998. The last ice
20 sheet in north-west Scotland: reconstruction and implications. *Quaternary Science*
21 *Reviews* **17**, 1149-1184.
- 22 Bassett, S. E., Milne, G. A., Mitrovica, J. X. & Clark, P. U. 2005. Ice sheet and solid earth
23 influences on far-field sea-level histories. *Science* **309**, 925-928.

- 1 Béjar-Pizarro, M., Socquet, A., Armijo, R., Carrizo, D., Genrich, J. & Simons, M. 2013.
2 Andean structural control on interseismic coupling in the North Chile subduction zone.
3 *Nature Geoscience* **6**, 462-467.
- 4 Bekaert, D. P., Hooper, A. J. & Wright, T. J. 2015. A spatially variable power law
5 tropospheric correction technique for InSAR data. *Journal of Geophysical Research:*
6 *Solid Earth* **120**, 1345-1356.
- 7 Berardino, P., Fornaro, G., Lanari, R. & Sansosti, E. 2002. A new algorithm for surface
8 deformation monitoring based on small baseline differential SAR interferograms. *IEEE*
9 *Transactions on Geoscience and Remote Sensing* **40**, 2375-2383.
- 10
- 11 Biggs, J., Wright, T., Lu, Z. & Parsons, B. 2007. Multi-interferogram method for measuring
12 interseismic deformation: Denali Fault, Alaska. *Geophysical Journal International* **170**,
13 1165-1179.
- 14 Bingley, R. M., Dodson, A., Penna, N., Teferle, F. N. & Baker, T. 2001. Monitoring the
15 vertical land movement component of changes in mean sea level using GPS: results
16 from tide gauges in the UK. *Journal of Geospatial Engineering* **3**, 9-20.
- 17 Bingley, R. M., Teferle, F. N., Orliac, E. J., Dodson, A. H., Williams, S. D. P., Blackman, D.
18 L., Baker, T. F., Riedmann, M., Haynes, M., Aldiss, D. T., Burke, H. C., Chacksfield, B.
19 C. & Tragheim, D. G. 2007. Absolute fixing of tide gauge benchmarks and land levels:
20 Measuring changes in land and sea levels around the coast of Great Britain and along
21 the Thames Estuary and River Thames using GPS, Absolute Gravimetry, Persistent
22 Scatterer Interferometry and tide gauges. *R&D Technical Report FD2319/TR, Joint*
23 *Defra/EA Flood and Coastal Erosion Risk Management R&D Programme*.

- 1 Blewitt, G. 2003. Self-consistency in reference frames, geocenter definition, and surface
2 loading of the solid Earth. *Journal of Geophysical Research: Solid Earth* (1978–2012)
3 **108**.
- 4 Blewitt, G. & Lavallée, D. 2002. Effect of annual signals on geodetic velocity. *Journal of*
5 *Geophysical Research: Solid Earth* (1978–2012) **107**, ETG 9-1-ETG 9-11.
- 6 Blewitt, G., Altamimi, Z., Davis, J., Gross, R., Kuo, C.-Y., Lemoine, F. G., Moore, A. W.,
7 Neilan, R. E., Plag, H.-P. & Rothacher, M. 2010. Geodetic observations and global
8 reference frame contributions to understanding sea-level rise and variability. *In* Church,
9 J. A., Woodworth, P. L., Aarup, T. & Wilson, W. S. (eds) *Understanding Sea-Level*
10 *Rise and Variability*, 256-284. London: Wiley-Blackwell.
- 11 Bradley, S. L., Milne, G. A., Zong, Y. & Horton, B. 2008. Modelling sea-level data from
12 China and Malay-Thai Peninsula to infer Holocene eustatic sea-level change. *AGU Fall*
13 *Meeting Abstracts*, 0763.
- 14 Bradley, S. L., Milne, G. A., Teferle, F. N., Bingley, R. M. & Orliac, E. J. 2009. Glacial
15 isostatic adjustment of the British Isles: new constraints from GPS measurements of
16 crustal motion. *Geophysical Journal International* **178**, 14-22.
- 17 Bradley, S. L., Milne, G. A., Shennan, I. & Edwards, R. J. 2011. An improved glacial
18 isostatic adjustment model for the British Isles. *Journal of Quaternary Science* **26**, 541-
19 552.
- 20 British Isles continuous GNSS Facility (BIGF) 2014. The creation of a map of current
21 vertical land movements in the UK, based on absolute gravity and CGPS. Electronic
22 Article <http://www.bigf.ac.uk/files/papers/Bingley_SOFI_NEF0121791_Report.pdf>
23 [Date accessed: 13.07.2015].
- 24 British Isles continuous GNSS Facility (BIGF) 2015. Data derived based on archived raw
25 data from continuous GNSS stations in the British Isles for the period from March 1997

- June 2014. Created by D. N. Hansen and R. M. Bingley, Natural Environment Research Council (NERC) British Isles continuous GNSS Facility (BIGF), University of Nottingham, UK. Data set accessed 2015-03-04 at <http://www.bigf.ac.uk>.
- Brooks, A. J., Bradley, S. L., Edwards, R. J., Milne, G. A., Horton, B. & Shennan, I. 2008. Postglacial relative sea-level observations from Ireland and their role in glacial rebound modelling. *Journal of Quaternary Science* **23**, 175-192.
- Brooks, B. A., Merrifield, M. A., Foster, J., Werner, C. L., Gomez, F., Bevis, M. & Gill, S. 2007. Space geodetic determination of spatial variability in relative sea level change, Los Angeles basin. *Geophysical Research Letters* **34**.
- Carbognin, L., Teatini, P. & Tosi, L. 2004. Eustacy and land subsidence in the Venice Lagoon at the beginning of the new millennium. *Journal of Marine Systems* **51**, 345-353.
- Carter, W. E. 1994. Report of the Surrey workshop of the IAPSO tide gauge bench mark fixing committee, held at the Institute of Oceanographic Sciences, UK. NOAA Technical Report, NOSOES0006.
- Carter, W. E., Aubrey, D. G., Baker, T., Boucher, C., LeProvost, C., Pugh, D. T., Peltier, W. R., Zumberge, M. A., Rapp, R. H. & Schultz, R. E. 1989. Geodetic fixing of tide gauge bench marks: technical report. Woods Hole Oceanographic Institution.
- Castillo, M., Bishop, P. & Jansen, J. D. 2013. Knickpoint retreat and transient bedrock channel morphology triggered by base-level fall in small bedrock river catchments: The case of the Isle of Jura, Scotland. *Geomorphology* **180-181**, 1-9.
- Chen, Q., Liu, G., Ding, X., Hu, J.-C., Yuan, L., Zhong, P. & Omura, M. 2010. Tight integration of GPS observations and persistent scatterer InSAR for detecting vertical ground motion in Hong Kong. *International Journal of Applied Earth Observation and Geoinformation* **12**, 477-486.

- 1 Cigna, F., Bateson, L., Jordan, C. & Dashwood, C. 2012. Feasibility of InSAR technologies
2 for nationwide monitoring of geohazards in Great Britain. *RSPSoc 2012* , London, UK,
3 12-14 Sept 2012.
- 4 Cigna, F., Bateson, L., Jordan, C. & Dashwood, C. 2013. Nationwide monitoring of
5 geohazards in Great Britain with InSAR: Feasibility mapping based on ERS-1/2 and
6 ENVISAT imagery. *IEEE International Geoscience and Remote Sensing*
7 *Symposium, IGARSS 2013*, 672-675.
- 8 Cigna, F., Bateson, L., Jordan, C. & Dashwood, C. 2014a. Simulating SAR geometric
9 distortions and predicting Persistent Scatterer densities for ERS-1/2 and ENVISAT C-
10 band SAR and InSAR applications: Nationwide feasibility assessment to monitor the
11 landmass of Great Britain with SAR imagery. *Remote Sensing of Environment* **152**, 441-
12 466.
- 13 Cigna, F., Rawlins, B. G., Jordan, C., Sowter, A. & Evans, C. 2014b. Intermittent Small
14 Baseline Subset (ISBAS) InSAR of rural and vegetated terrain: a new method to
15 monitor land motion applied to peatlands in Wales, UK. *Geophysical Research*
16 *Abstracts 16, EGU2014-3844-1, EGU General Assembly 2014*
- 17 Clark, J. A., Farrell, W. E. & Peltier, W. R. 1978. Global changes in postglacial sea level: a
18 numerical calculation. *Quaternary Research* **9**, 265-287.
- 19 Collilieux, X. & Altamimi, Z. 2013. External Evaluation of the Origin and Scale of the
20 International Terrestrial Reference Frame. In Sideris, M. G. (ed) *Reference Frames for*
21 *Applications in Geosciences*, 27-31. Springer.
- 22 Costantini, M., Falco, S., Malvarosa, F. & Minati, F. 2008. A new method for identification
23 and analysis of persistent scatterers in series of SAR images. *IEEE International*
24 *Geoscience and Remote Sensing Symposium, IGARSS 2008.*, II-449-II-452.

- 1 Crosetto, M., Crippa, B., Biescas, E., Monserrat, O. & Agudo, M. 2005. State of the art of
2 land deformation monitoring using differential SAR interferometry. *ISPRS Hannover*
3 *Workshop 2005: High Resolution Earth Imaging for Geospatial Information*, 17-20.
- 4 Cullingford, R. A., Smith, D. E. & Firth, C. R. 1991. The altitude and age of the Main
5 Postglacial Shoreline in eastern Scotland. *Quaternary International* **9**, 39-52.
- 6 Davenport, C. A. & Ringrose, P. S. 1985. Fault activity and palaeoseismicity during
7 Quaternary time in Scotland – preliminary studies. *Earthquake Engineering in Britain*,
8 143-155. London, UK: Thomas Telford Ltd.
- 9 Davenport, C. A., Ringrose, P. S., Becker, A., Hancock, P. & Fenton, C. 1989. Geological
10 investigations of late and post glacial earthquake activity in Scotland. In Gregersen, S.,
11 Basham, P. W. (eds) *Earthquakes at North Atlantic Passive Margins: Neotectonics and*
12 *Postglacial Rebound* 175-194. Dordrecht, The Netherlands: Kluwer Academic
13 Publishers.
- 14 Dawson, A. G. 1979. *Raised shorelines of Jura, Scarba and NE Islay*. Doctoral Dissertation,
15 University of Edinburgh, UK
- 16 Dawson, A. G. 1980. The low rock platform in western Scotland. *Proceedings of the*
17 *Geologists' Association* **91**, 339-344.
- 18 Dawson, A. G. 1984. Quaternary sea-level changes in western Scotland. *Quaternary Science*
19 *Reviews* **3**, 345-368.
- 20 Dawson, A. G., Bondevik, S. & Teller, J. T. 2011. Relative timing of the Storegga submarine
21 slide, methane release, and climate change during the 8.2 ka cold event. *The Holocene*
22 **21**, 1167-1171.
- 23 Dong, D., Yunc, T. & Heflin, M. 2003. Origin of the international terrestrial reference
24 frame. *Journal of Geophysical Research: Solid Earth (1978–2012)* **108**.

- 1 Dong, D., Fang, P., Bock, Y., Webb, F., Prawirodirdjo, L., Kedar, S. & Jamason, P. 2006.
2 Spatiotemporal filtering using principal component analysis and Karhunen-Loeve
3 expansion approaches for regional GPS network analysis. *Journal of Geophysical*
4 *Research: Solid Earth (1978–2012)* **111**.
- 5 Fairbridge, R. W. 1961. Eustatic changes in sea level. *Physics and Chemistry of the Earth* **4**,
6 99-185.
- 7 Fan, H., Deng, K., Ju, C., Zhu, C. & Xue, J. 2011. Land subsidence monitoring by D-InSAR
8 technique. *Mining Science and Technology (China)* **21**, 869-872.
- 9 Farrell, W. E. & Clark, J. A. 1976. On Postglacial Sea Level. *Geophysical Journal of the*
10 *Royal Astronomical Society* **46**, 647-667.
- 11 Feng, W. 2014. *Modelling co- and post-seismic displacements revealed by InSAR and their*
12 *implications for fault behaviour*. Doctoral Dissertation, School of Geographical and
13 Earth Sciences, University of Glasgow, UK.
- 14 Feng, W., Li, Z., Hoey, T., Zhang, Y., Wang, R., Samsonov, S., Li, Y. & Xu, Z. 2014.
15 Patterns and mechanisms of coseismic and postseismic slips of the 2011 M W 7.1 Van
16 (Turkey) earthquake revealed by multi-platform synthetic aperture radar interferometry.
17 *Tectonophysics* **632**, 188-198.
- 18 Ferretti, A., Prati, C. & Rocca, F. 2000. Nonlinear subsidence rate estimation using
19 permanent scatterers in differential SAR interferometry. *IEEE Transactions on*
20 *Geoscience and Remote Sensing* **38**, 2202-2212.
- 21 Ferretti, A., Prati, C. & Rocca, F. 2001. Permanent scatterers in SAR interferometry. *IEEE*
22 *Transactions on Geoscience and Remote Sensing* **39**, 8-20.
- 23 Firth, C. R. 1984. *Raised shorelines and ice limits in the inner Moray Firth and Loch Ness*
24 *areas, Scotland*. Doctoral Dissertation, Coventry (Lanchester) Polytechnic, UK.

- 1 Firth, C. R. 1986. Isostatic depression during the Loch Lomond Stadial: preliminary evidence
2 from the Great Glen, northern Scotland. *Quaternary Newsletter* **48**, 1-9.
- 3 Firth, C. R. 1992. Loch Ness Shorelines: evidence for isostatic depression during the Loch
4 Lomond (Younger Dryas) Stadial. In Fenton, C. (ed) *Neotectonics in Scotland: A Field*
5 *Guide*, 72-75. University of Glasgow, Glasgow.
- 6 Firth, C. R. & Haggart, B. A. 1989. Loch Lomond stadial and Flandrian shorelines in the
7 inner Moray Firth area, Scotland. *Journal of Quaternary Science* **4**, 37-50.
- 8 Firth, C. R. & Stewart, I. S. 2000. Postglacial tectonics of the Scottish glacio-isostatic uplift
9 centre. *Quaternary Science Reviews* **19**, 1469-1493.
- 10 Firth, C. R., Smith, D. E. & Cullingford, R. A. 1993. Late Devensian and Holocene glacio-
11 isostatic uplift patterns in Scotland. *Quaternary Proceedings*, **14**.
- 12 Firth, C. R., Smith, D. E., Hansom, J. D. & Pearson, S. G. 1995. Holocene spit development
13 on a regressive shoreline, Dornoch Firth, Scotland. *Marine Geology* **124**, 203-214.
- 14 Fleming, K., Johnston, P., Zwartz, D., Yokoyama, Y., Lambeck, K. & Chappell, J. 1998.
15 Refining the eustatic sea-level curve since the Last Glacial Maximum using far- and
16 intermediate-field sites. *Earth and Planetary Science Letters* **163**, 327-342.
- 17 Forsberg, R., Sideris, M. G. & Shum, C. K. 2005. The gravity field and GGOS. *Journal of*
18 *Geodynamics* **40**, 387-393.
- 19 Fournier, T., Pritchard, M. E. & Finnegan, N. 2011. Accounting for atmospheric delays in
20 InSAR data in a search for long-wavelength deformation in South America. *IEEE*
21 *Transactions on Geoscience and Remote Sensing* **49**, 3856-3867.
- 22 Fretwell, P., Peterson, I. R. & Smith, D. E. 2004. The use of Gaussian trend surfaces for
23 modelling glacio-isostatic crustal rebound. *Scottish Journal of Geology* **40**, 175-179.

- 1 Fretwell, P. T., Smith, D. E. & Harrison, S. 2008. The Last Glacial Maximum British-Irish
2 Ice Sheet: a reconstruction using Digital Terrain Mapping. *Journal of Quaternary*
3 *Science* **23**, 241-248.
- 4 Gourmelen, N., Amelung, F. & Lanari, R. 2010. Interferometric synthetic aperture radar–
5 GPS integration: Interseismic strain accumulation across the Hunter Mountain fault in
6 the eastern California shear zone. *Journal of Geophysical Research: Solid Earth* (1978–
7 2012) **115**.
- 8 Gray, J. M. 1974. The Main Rock Platform of the Firth of Lorn, western Scotland.
9 *Transactions of the Institute of British Geographers* **61**, 81-99.
- 10 Gray, J. M. 1978. Low level shore platforms in the south-west Scottish Highlands.
11 *Transactions of the Institute of British Geographers* **3**, 151-164.
- 12 Greaves, M., Bingley, R. M., Baker, D. F., Hansen, D. N., Sherwood, R. & Clarke, P. 2013.
13 National Report of Great Britain 2013. *EUREF Symposium, Budapest, Hungary, June*
14 *2013*.
- 15 Greaves, M., Bingley, R. M., Baker, D. F., Hansen, D. N. & Clarke, P. 2015. [National Report](#)
16 [of Great Britain 2015](#). *EUREF Symposium, Leipzig, Germany, 2015*.
- 17 Hammond, W. C., Blewitt, G., Li, Z., Plag, H.-P. & Kreemer, C. 2012. Contemporary uplift
18 of the Sierra Nevada, western United States, from GPS and InSAR measurements.
19 *Geology* **40**, 667-670.
- 20 Hansen, D. N., Teferle, F. N., Bingley, R. M. & Williams, S. D. P. 2012. New estimates of
21 present-day crustal/land motions in the British Isles based on the BIGF network. In
22 Kenyon, S., Pacino, M. C., Marti, U. (eds) *Geodesy for Planet Earth*, 665-671. Springer.
- 23 Hanssen, R. F. 2001. *Radar interferometry: data interpretation and error analysis*, 2.
24 Springer Science & Business Media.

- 1 Hill, E. M., Davis, J. L., Tamisiea, M. E. & Lidberg, M. 2010. Combination of geodetic
2 observations and models for glacial isostatic adjustment fields in Fennoscandia. *Journal*
3 *of Geophysical Research: Solid Earth (1978–2012)* **115**.
- 4 Hoffmann, J., Zebker, H. A., Galloway, D. L. & Amelung, F. 2001. Seasonal subsidence and
5 rebound in Las Vegas Valley, Nevada, observed by synthetic aperture radar
6 interferometry. *Water Resources Research* **37**, 1551-1566.
- 7 Hooper, A., Zebker, H., Segall, P. & Kampes, B. 2004. A new method for measuring
8 deformation on volcanoes and other natural terrains using InSAR persistent scatterers.
9 *Geophysical Research Letters* **31**.
- 10 Hooper, A., Bekaert, D., Spaans, K. & Arikan, M. 2012. Recent advances in SAR
11 interferometry time series analysis for measuring crustal deformation. *Tectonophysics*
12 **514**, 1-13.
- 13 James, T. S. & Lambert, A. 1993. A comparison of VLBI data with the Ice-3G Glacial
14 Rebound Model. *Geophysical Research Letters* **20**.
- 15 Jardine, W. G. 1980. Holocene raised coastal sediments and former shorelines in
16 Dumfriesshire and eastern Galloway. *Transactions of the Dumfries Natural History and*
17 *Antiquarian Society, series 3*, **55**, 1-59.
- 18 Johansson, J. M., Davis, J. L., Scherneck, H. G., Milne, G. A., Vermeer, M., Mitrovica, J. X.,
19 Bennett, R. A., Jonsson, B., Elgered, G., Elosegui, P., Koivula, H., Poutanen, M.,
20 Ronnang, B. O. & Shapiro, I. I. 2002. Continuous GPS measurements of postglacial
21 adjustment in Fennoscandia - 1. Geodetic results. *Journal of Geophysical Research-*
22 *Solid Earth* **107**.
- 23 Jordan, J. T., Smith, D. E., Dawson, S. & Dawson, A. G. 2010. Holocene relative sea-level
24 changes in Harris, Outer Hebrides, Scotland, UK. *Journal of Quaternary Science* **25**,
25 115-134.

- Kaneko, Y., Fialko, Y., Sandwell, D. T., Tong, X. & Furuya, M. 2013. Interseismic deformation and creep along the central section of the North Anatolian fault (Turkey): InSAR observations and implications for rate-and-state friction properties. *Journal of Geophysical Research: Solid Earth* **118**, 316-331.
- Kemp, D. D. 1976. Buried raised beaches on the northern side of the Forth valley, central Scotland. *Scottish Geographical Magazine* **92**, 120-128.
- Kuchar, J., Milne, G., Hubbard, A., Patton, H., Bradley, S., Shennan, I. & Edwards, R. 2012. Evaluation of a numerical model of the British–Irish ice sheet using relative sea-level data: implications for the interpretation of trimline observations. *Journal of Quaternary Science* **27**, 597-605.
- Lambeck, K. 1991. Glacial rebound and sea-level change in the British Isles. *Terra Nova* **3**, 379-389.
- Lambeck, K. 1993a. Glacial rebound of the British Isles—I. Preliminary model results. *Geophysical Journal International* **115**, 941-959.
- Lambeck, K. 1993b. Glacial rebound of the British Isles—II. A high-resolution, high-precision model. *Geophysical Journal International* **115**, 960-990.
- Lambeck, K. 1995. Late Devensian and Holocene shorelines of the British Isles and North Sea from models of glacio-hydro-isostatic rebound. *Journal of the Geological Society-London* **152**, 437-448.
- Lambeck, K. & Johnston, P. 1998. The Viscosity of the Mantle: Evidence from Analyses of Glacial-Rebound Phenomena. In Jackson, I. (ed) *The Earth's Mantle: Composition, Structure, and Evolution*, 461-502. Cambridge, UK: Cambridge University Press.
- Lambeck, K., Johnston, P., Smither, C. & Nakada, M. 1996. Glacial rebound of the British Isles-III. Constraints on mantle viscosity. *Geophysical Journal International* **125**, 340-354.

- 1 Lambeck, K., Smither, C. & Johnston, P. 1998. Sea-level change, glacial rebound and mantle
2 viscosity for northern Europe. *Geophysical Journal International* **134**, 102-144.
- 3 Lambert, A., Courtier, N., Sasagawa, G. S., Klopping, F., Winester, D., James, T. S. & Liard,
4 J. O. 2001. New constraints on Laurentide postglacial rebound from absolute gravity
5 measurements. *Geophysical Research Letters* **28**, 2109-2112.
- 6 Lambert, A., Courtier, N. & James, T. S. 2006. Long-term monitoring by absolute
7 gravimetry: Tides to postglacial rebound. *Journal of Geodynamics* **41**, 307-317.
- 8 Lanari, R., Mora, O., Manunta, M., Mallorquí, J. J., Berardino, P. & Sansosti, E. 2004. A
9 small-baseline approach for investigating deformations on full-resolution differential
10 SAR interferograms. *IEEE Transactions on Geoscience and Remote Sensing* **42**, 1377-
11 1386.
- 12 Lanari, R., Casu, F., Manzo, M., Zeni, G., Berardino, P., Manunta, M. & Pepe, A. 2007. An
13 overview of the small baseline subset algorithm: A DInSAR technique for surface
14 deformation analysis. *Pure and Applied Geophysics* **164**, 637-661.
- 15 Larson, K. M. & van Dam, T. 2000. Measuring postglacial rebound with GPS and absolute
16 gravity. *Geophysical Research Letters* **27**, 3925-3928.
- 17 Leighton, J. M., Sowter, A., Tragheim, D. G., Bingley, R. M. & Teferle, F. N. 2013. Land
18 motion in the urban area of Nottingham observed by ENVISAT-1. *International*
19 *Journal of Remote Sensing* **34**, 982-1003.
- 20 Li, Z., Muller, J. P., Cross, P. & Fielding, E. J. 2005. Interferometric synthetic aperture radar
21 (InSAR) atmospheric correction: GPS, Moderate Resolution Imaging Spectroradiometer
22 (MODIS), and InSAR integration. *Journal of Geophysical Research: Solid Earth*
23 *(1978–2012)* **110**.

- 1 Li, Z., Fielding, E. J., Cross, P. & Muller, J. P. 2006. Interferometric synthetic aperture radar
2 atmospheric correction: medium resolution imaging spectrometer and advanced
3 synthetic aperture radar integration. *Geophysical Research Letters* **33**.
- 4 Li, Z., Fielding, E. J. & Cross, P. 2009. Integration of InSAR time-series analysis and water-
5 vapor correction for mapping postseismic motion after the 2003 Bam (Iran) earthquake.
6 *IEEE Transactions on Geoscience and Remote Sensing* **47**, 3220-3230.
- 7 Li, Z., Pasquali, P., Cantone, A., Singleton, A., Funning, G. & Forrest, D. 2012. MERIS
8 atmospheric water vapor correction model for wide swath interferometric synthetic
9 aperture radar. *IEEE Geoscience and Remote Sensing Letters* **9**, 257-261.
- 10 Lidberg, M., Johansson, J. M., Scherneck, H. G. & Davis, J. L. 2007. An improved and
11 extended GPS-derived 3D velocity field of the glacial isostatic adjustment (GIA) in
12 Fennoscandia. *Journal of Geodesy* **81**, 213-230.
- 13 Liu, D., Shao, Y., Liu, Z., Riedel, B., Sowter, A., Niemeier, W. & Bian, Z. 2014. Evaluation
14 of InSAR and TomoSAR for monitoring deformations caused by mining in a
15 mountainous area with high resolution satellite-based SAR. *Remote Sensing* **6**, 1476-
16 1495.
- 17 Lundgren, P., Hetland, E. A., Liu, Z. & Fielding, E. J. 2009. Southern San Andreas-San
18 Jacinto fault system slip rates estimated from earthquake cycle models constrained by
19 GPS and interferometric synthetic aperture radar observations. *Journal of Geophysical*
20 *Research: Solid Earth (1978–2012)* **114**.
- 21 MacMillan, D. S. 2004. Rate difference between VLBI and GPS reference frame scales. *AGU*
22 *Fall Meeting 2004 Abstracts*, #G21B-05.
- 23 MacMillan, D. S. & Boy, J.-P. 2004. Mass loading effects on crustal displacements measured
24 by VLBI. *International VLBI Service for Geodesy and Astrometry 2004 General*
25 *Meeting Proceedings*, 476.

- 1 Manzo, M., Fialko, Y., Casu, F., Pepe, A. & Lanari, R. 2012. A quantitative assessment of
2 DInSAR measurements of interseismic deformation: the Southern San Andreas Fault
3 case study. *Pure and Applied Geophysics* **169**, 1463-1482.
- 4 Marinkovic, P., Ketelaar, G., van Leijen, F. & Hanssen, R. 2008. InSAR quality control:
5 Analysis of five years of corner reflector time series. *Proceedings Fringe 2007*
6 *Workshop, Frascati, Italy*. European Space Agency (Special Publication) ESA SP-649,
7 26-30.
- 8 Massonnet, D. & Feigl, K. L. 1998. Radar interferometry and its application to changes in the
9 Earth's surface. *Reviews of Geophysics* **36**, 441-500.
- 10 Mccarroll, D. & Ballantyne, C. K. 2000. The last ice sheet in Snowdonia. *Journal of*
11 *Quaternary Science* **15**, 765-778.
- 12 McIntyre, K. L. & Howe, J. A. 2010. Scottish west coast fjords since the last glaciation: a
13 review. *Geological Society, London, Special Publications* **344**, 305-329.
- 14 Milne, G. A. & Mitrovica, J. X. 2008. Searching for eustasy in deglacial sea-level histories.
15 *Quaternary Science Reviews* **27**, 2292-2302.
- 16 Milne, G. A., Davis, J. L., Mitrovica, J. X., Scherneck, H. G., Johansson, J. M., Vermeer, M.
17 & Koivula, H. 2001. Space-geodetic constraints on glacial isostatic adjustment in
18 Fennoscandia. *Science* **291**, 2381-2385.
- 19 Milne, G. A., Mitrovica, J. X., Scherneck, H. G., Davis, J. L., Johansson, J. M., Koivula, H.
20 & Vermeer, M. 2004. Continuous GPS measurements of postglacial adjustment in
21 Fennoscandia: 2. Modeling results. *Journal of Geophysical Research-Solid Earth* **109**.
- 22 Milne, G. A., Shennan, I., Youngs, B. A. R., Waugh, A. I., Teferle, F. N., Bingley, R. M.,
23 Bassett, S. E., Cuthbert-Brown, C. & Bradley, S. L. 2006. Modelling the glacial isostatic
24 adjustment of the UK region. *Philosophical Transactions of the Royal Society A -*
25 *Mathematical Physical and Engineering Sciences* **364**, 931-948.

- 1 Mitrovica, J. X. & Milne, G. A. 2003. On post-glacial sea level: I. General theory.
2 *Geophysical Journal International* **154**, 253-267.
- 3 Mitrovica, J. X. & Peltier, W. R. 1989. Pleistocene deglaciation and the global gravity field.
4 *Journal of Geophysical Research: Solid Earth (1978–2012)* **94**, 13651-13671.
- 5 Mitrovica, J. X., Davis, J. L. & Shapiro, I. I. 1993. Constraining proposed combinations of
6 ice history and Earth rheology using VLBI determined baseline length rates in North
7 America. *Geophysical Research Letters* **20**, 2387-2390.
- 8 Niebauer, T. M., Sasagawa, G. S., Faller, J. E., Hilt, R. & Klopping, F. 1995. A new
9 generation of absolute gravimeters. *Metrologia* **32**, 159.
- 10 Ordnance Survey 2015. A guide to coordinate systems in Great Britain. An introduction to
11 mapping coordinate systems and the use of GPS datasets with Ordnance Survey
12 mapping. Version 2.4. Electronic Article
13 <[http://www.ordnancesurvey.co.uk/docs/support/guide-coordinate-systems-great-](http://www.ordnancesurvey.co.uk/docs/support/guide-coordinate-systems-great-britain.pdf)
14 [britain.pdf](http://www.ordnancesurvey.co.uk/docs/support/guide-coordinate-systems-great-britain.pdf)> [Date accessed 04.12.2015].
- 15 Osmanoglu, B., Dixon, T. H., Wdowinski, S., Cabral-Cano, E. & Jiang, Y. 2011. Mexico
16 City subsidence observed with persistent scatterer InSAR. *International Journal of*
17 *Applied Earth Observation and Geoinformation* **13**, 1-12.
- 18 Peltier, W. R. 1974. The impulse response of a Maxwell Earth. *Reviews of Geophysics and*
19 *Space Physics* **12**, 649-669.
- 20 Peltier, W. R. 1994. Ice age paleotopography. *Science* **265**, 195-201.
- 21 Peltier, W. R. 1995. VLBI baseline variations from the Ice-4G Model of postglacial rebound.
22 *Geophysical Research Letters* **22**, 465-468.
- 23 Peltier, W. R. 1996a. Global sea level rise and glacial isostatic adjustment: an analysis of data
24 from the east coast of North America. *Geophysical Research Letters* **23**, 717-720.

- 1 Peltier, W. R. 1996b. Mantle viscosity and ice-age ice sheet topography. *Science* **273**, 1359-
2 1364.
- 3 Peltier, W. R. 1998a. Postglacial variations in the level of the sea: Implications for climate
4 dynamics and solid-earth geophysics. *Reviews of Geophysics* **36**, 603-689.
- 5 Peltier, W. R. 1998b. The inverse problem for mantle viscosity. *Inverse Problems* **14**, 441.
- 6 Peltier, W. R. 2002. On eustatic sea level history: Last Glacial Maximum to Holocene.
7 *Quaternary Science Reviews* **21**, 377-396.
- 8 Peltier, W. R. 2004. Global glacial isostasy and the surface of the ice-age Earth: the ICE-5G
9 (VM2) model and GRACE. *Annual Review of Earth and Planetary Sciences* **32**, 111-
10 149.
- 11 Peltier, W. R. & Andrews, J. T. 1976. Glacial-isostatic adjustment—I. The forward problem.
12 *Geophysical Journal International* **46**, 605-646.
- 13 Peltier, W. R. & Jiang, X. 1996. Glacial isostatic adjustment and Earth rotation: Refined
14 constraints on the viscosity of the deepest mantle. *Journal of Geophysical Research:*
15 *Solid Earth (1978–2012)* **101**, 3269-3290.
- 16 Peltier, W. R., Shennan, I., Drummond, R. & Horton, B. 2002. On the postglacial isostatic
17 adjustment of the British Isles and the shallow viscoelastic structure of the Earth.
18 *Geophysical Journal International* **148**, 443-475.
- 19 Plag, H. P., Axe, P., Knudsen, P., Richter, B. & Verstraeten, J. 2000. European sea level
20 observing system (EOSS). *Status and future developments, COST Action*, **40**.
- 21 Prawirodirdjo, L. & Bock, Y. 2004. Instantaneous global plate motion model from 12 years
22 of continuous GPS observations. *Journal of Geophysical Research: Solid Earth (1978–*
23 *2012)* **109**.

- 1 Pritchard, M. E., Ji, C. & Simons, M. 2006. Distribution of slip from 11 Mw> 6 earthquakes
2 in the northern Chile subduction zone. *Journal of Geophysical Research: Solid Earth*
3 (1978–2012) **111**.
- 4 Remy, D., Chen, Y., Froger, J. L., Bonvalot, S., Cordoba, M. & Fustos, J. 2015. Revised
5 interpretation of recent InSAR signals observed at Llaima volcano (Chile). *Geophysical*
6 *Research Letters* **42**, 3870–3879.
- 7 Rennie, A. F. & Hansom, J. D. 2011. Sea level trend reversal: Land uplift outpaced by sea
8 level rise on Scotland's coast. *Geomorphology* **125**, 193-202.
- 9 Ringrose, P. S. 1987. *Fault activity and palaeoseismicity during Quaternary time in Scotland*.
10 Doctoral Dissertation, University of Strathclyde, UK.
- 11 Ringrose, P. S. 1989. Palaeoseismic (?) liquefaction event in late Quaternary lake sediments
12 at Glen Roy, Scotland. *Terra Nova* **1**, 57-62.
- 13 Ringrose, P. S., Hancock, P. L., Fenton, C. & Davenport, C. A. 1991. Quaternary tectonic
14 activity in Scotland. In Foster, A., Culshaw, M. G., Cripps, J. C., Little, J. A., Moon, C.
15 F. (eds) *Quaternary Engineering Geology*. Engineering Geology Special Publication **7**,
16 679-686. London, UK: The Geological Society.
- 17 Rosen, P. A., Hensley, S., Zebker, H. A., Webb, F. H. & Fielding, E. J. 1996. Surface
18 deformation and coherence measurements of Kilauea Volcano, Hawaii, from SIR-C
19 radar interferometry. *Journal of Geophysical Research* **101**, 23,109-23,125.
- 20 Samsonov, S. & d'Orey, N. 2012. Multidimensional time-series analysis of ground
21 deformation from multiple InSAR data sets applied to Virunga Volcanic Province.
22 *Geophysical Journal International* **191**, 1095-1108.
- 23 Sanli, D. U. & Blewitt, G. 2001. Geocentric sea level trend using GPS and >100-year tide
24 gauge record on a postglacial rebound nodal line. *Journal of Geophysical Research:*
25 *Solid Earth (1978–2012)* **106**, 713-719.

- Sasgen, I., Martinec, Z. & Bamber, J. 2010. Combined GRACE and InSAR estimate of West Antarctic ice mass loss. *Journal of Geophysical Research: Earth Surface* (2003–2012) **115**.
- Selby, K. A. & Smith, D. E. 2007. Late Devensian and Holocene relative sea-level changes on the Isle of Skye, Scotland, UK. *Journal of Quaternary Science* **22**, 119-139.
- Shakun, J. D. & Carlson, A. E. 2010. A global perspective on Last Glacial Maximum to Holocene climate change. *Quaternary Science Reviews* **29**, 1801-1816.
- Shennan, I. 1982. Interpretation of Flandrian sea-level data from the Fenland, England. *Proceedings of the Geologists' Association* **93**, 53-63.
- Shennan, I. 1983. Flandrian and Late Devensian sea-level changes and crustal movements in England and Wales. In *Shorelines and isostasy* **16**, 255-283. London: Academic Press .
- Shennan, I. 1986a. Flandrian sea-level changes in the Fenland. I: The geographical setting and evidence of relative sea-level changes. *Journal of Quaternary Science* **1**, 119-153.
- Shennan, I. 1986b. Flandrian sea-level changes in the Fenland. II: Tendencies of sea-level movement, altitudinal changes, and local and regional factors. *Journal of Quaternary Science* **1**, 155-179.
- Shennan, I. 1987. Global analysis and correlation of sea-level data. In Devoy, R. J. N. (ed) *Sea Surface Studies*, 198-230. Springer.
- Shennan, I. 1989. Holocene crustal movements and sea-level changes in Great Britain. *Journal of Quaternary Science* **4**, 77-89.
- Shennan, I. 1992. Late Quaternary sea-level changes and crustal movements in eastern England and eastern Scotland: an assessment of models of coastal evolution. *Quaternary International* **15**, 161-173.
- Shennan, I. 1999. Global meltwater discharge and the deglacial sea-level record from northwest Scotland. *Journal of Quaternary Science* **14**, 715-719.

- Shennan, I. 2015. Handbook of sea-level research: framing research questions. *In* Shennan, I., Long, A. J. & Horton, B. P. (eds) *Handbook of Sea-Level Research*. Chichester, UK: John Wiley & Sons, Ltd.
- Shennan, I. & Horton, B. 2002. Holocene land- and sea-level changes in Great Britain. *Journal of Quaternary Science* **17**, 511-526.
- Shennan, I., Tooley, M. J., Davis, M. J. & Haggart, B. A. 1983. Analysis and interpretation of Holocene sea-level data. *Nature* **302**, 404 – 406.
- Shennan, I., Innes, J. B., Long, A. J. & Zong, Y. 1993. Late Devensian and Holocene relative sea-level changes at Rumach, near Arisaig, northwest Scotland. *Norsk Geologisk Tidsskrift* **73**, 161-174.
- Shennan, I., Innes, J. B., Long, A. J. & Zong, Y. 1994. Late Devensian and Holocene relative sealevel changes at Loch nan Eala, near Arisaig, northwest Scotland. *Journal of Quaternary Science* **9**, 261-283.
- Shennan, I., Innes, J. B., Long, A. J. & Zong, Y. 1995a. Late Devensian and Holocene relative sea-level changes in northwestern Scotland: new data to test existing models. *Quaternary International* **26**, 97-123.
- Shennan, I., Innes, J. B., Long, A. J. & Zong, Y. 1995b. Holocene relative sea-level changes and coastal vegetation history at Kentra Moss, Argyll, northwest Scotland. *Marine Geology* **124**, 43-59.
- Shennan, I., Lambeck, K., Horton, B., Innes, J. B., Lloyd, J., McArthur, J., Purcell, T. & Rutherford, M. 2000. Late Devensian and Holocene records of relative sea-level changes in northwest Scotland and their implications for glacio-hydro-isostatic modelling. *Quaternary Science Reviews* **19**, 1103-1135.

- 1 Shennan, I., Peltier, W. R., Drummond, R. & Horton, B. 2002. Global to local scale
2 parameters determining relative sea-level changes and the post-glacial isostatic
3 adjustment of Great Britain. *Quaternary Science Reviews* **21**, 397-408.
- 4 Shennan, I., Hamilton, S., Hillier, C. & Woodroffe, S. 2005. A 16000-year record of near-
5 field relative sea-level changes, northwest Scotland, United Kingdom. *Quaternary*
6 *International* **133**, 95-106.
- 7 Shennan, I., Bradley, S. L., Milne, G., Brooks, A., Bassett, S. & Hamilton, S. 2006a. Relative
8 sea-level changes, glacial isostatic modelling and ice-sheet reconstructions from the
9 British Isles since the Last Glacial Maximum. *Journal of Quaternary Science* **21**, 585-
10 599.
- 11 Shennan, I., Hamilton, S., Hillier, C., Hunter, A., Woodall, R., Bradley, S. L., Milne, G.,
12 Brooks, A. & Bassett, S. 2006b. Relative sea-level observations in western Scotland
13 since the Last Glacial Maximum for testing models of glacial isostatic land movements
14 and ice-sheet reconstructions. *Journal of Quaternary Science* **21**, 601-613.
- 15 Shennan, I., Milne, G. & Bradley, S. L. 2009. Late Holocene relative land- and sea-level
16 changes: Providing information for stakeholders. *GSA Today* **19**.
- 17 Shennan, I., Milne, G. & Bradley, S. L. 2012. Late Holocene vertical land motion and relative
18 sea-level changes: lessons from the British Isles. *Journal of Quaternary Science* **27**, 64-
19 70.
- 20 Singleton, A., Li, Z., Hoey, T. & Muller, J.-P. 2014. Evaluating sub-pixel offset techniques as
21 an alternative to D-InSAR for monitoring episodic landslide movements in vegetated
22 terrain. *Remote Sensing of Environment* **147**, 133-144.
- 23 Sissons, J. B. 1962. A re-interpretation of the literature on late-glacial shorelines in Scotland
24 with particular reference to the Forth area. *Transactions of the Edinburgh Geological*
25 *Society* **19**, 83-99.

- 1 Sissons, J. B. 1963. Scottish raised shoreline heights with particular reference to the Forth
2 valley. *Geografiska Annaler* **45**, 180-185.
- 3 Sissons, J. B. 1966. Relative sea level changes between 10300 and 8300 BP in part of the
4 Carse of Stirling. *Transactions of the Institute of British Geographers* **39**, 19-29.
- 5 Sissons, J. B. 1969. Drift stratigraphy and buried morphological features in the Grangemouth-
6 Falkirk-Airth area, central Scotland. *Transactions of the Institute of British*
7 *Geographers* **48**, 19-50.
- 8 Sissons, J. B. 1972. Dislocation and non-uniform uplift of raised shorelines in the western
9 part of the Forth valley. *Transactions of the Institute of British Geographers* **55**, 145-
10 159.
- 11 Sissons, J. B. 1983. Shorelines and isostasy in Scotland. In *Shorelines and isostasy* **16**, 209-
12 225. London: Academic Press.
- 13 Sissons, J. B. In Press. The lateglacial lakes of Glens Roy, Spean and vicinity (Lochaber
14 district, Scottish Highlands). *Proceedings of the Geologists' Association*.
- 15 Sissons, J. B. & Cornish, R. 1982. Differential Glacio-Isostatic Uplift of Crustal Blocks at
16 Glen Roy, Scotland. *Quaternary Research* **18**, 268-288.
- 17 Sissons, J. B., Smith, D. E. & Cullingford, R. A. 1966. Late-glacial and post-glacial
18 shorelines in South-East Scotland. *Transactions of the Institute of British Geographers*
19 **39**, 9-18.
- 20 Smith, D. E. 1968. Post-glacial displaced shorelines on the northern bank of the River Forth,
21 in Scotland. *Zeitschrift für Geomorphologie* **NF12** (4), 388-408.
- 22 Smith, D. E. 2005. Evidence for secular sea surface level changes in the Holocene raised
23 shorelines of Scotland, UK. *Journal of Coastal Research* **42**, 26-42.

- 1 Smith, D. E., Sissons, J. B. & Cullingford, R. A. 1969. Isobases for the Main Perth raised
2 shoreline in South East Scotland as determined by trend-surface analysis. *Institute of*
3 *British Geographers Transactions* **46**, 45-52.
- 4 Smith, D. E., Thompson K. S. R. & Kemp, D. E. 1978. The Late Devensian and Flandrian
5 History of the Teith valley. *Boreas* **7**, 97-107.
- 6 Smith, D. E., Morrison, J., Jones, R. L. & Cullingford, R. A. 1980. Dating the main
7 postglacial shoreline in the Montrose area, Scotland. In *Timescales in geomorphology*,
8 225-245. Chichester: Wiley .
- 9 Smith, D. E., Firth, C. R., Turbayne, S. C. & Brooks, C. L. 1992. Holocene relative sea-level
10 changes and shoreline displacement in the Dornoch Firth area, Scotland. *Proceedings of*
11 *the Geologists' Association* **103**, 237-257.
- 12 Smith, D. E., Firth, C. R., Brooks, C. L., Robinson, M. & Collins, P. E. F. 1999. Relative sea-
13 level rise during the Main Postglacial Transgression in NE Scotland, UK. *Transactions*
14 *of the Royal Society of Edinburgh: Earth Sciences* **90**, 1-27.
- 15 Smith, D. E., Cullingford, R. A. & Firth, C. R. 2000. Patterns of isostatic land uplift during
16 the Holocene: evidence from mainland Scotland. *Holocene* **10**, 489-501.
- 17 Smith, D. E., Firth, C. R. & Cullingford, R. A. 2002. Relative sea-level trends during the
18 early-middle Holocene along the eastern coast of mainland Scotland, UK. *Boreas* **31**,
19 185-202.
- 20 Smith, D. E., Haggart, B. A., Cullingford, R. A., Tipping, R. M., Wells, J. M., Mighall, T. M.
21 & Dawson, S. 2003a. Holocene relative sea-level change in the lower Nith valley and
22 estuary. *Scottish Journal of Geology* **39**, 97-120.
- 23 Smith, D. E., Wells, J. M., Mighall, T. M., Cullingford, R. A., Holloway, L. K., Dawson, S.
24 & Brooks, C. L. 2003b. Holocene relative sea levels and coastal changes in the lower

- 1 Cree valley and estuary, SW Scotland, UK. *Transactions of the Royal Society of*
2 *Edinburgh: Earth Sciences* **93**, 301-331.
- 3 Smith, D. E., Shi, S., Cullingford, R. A., Dawson, A. G., Dawson, S., Firth, C. R., Foster, I.
4 D. L., Fretwell, P. T., Haggart, B. A. & Holloway, L. K. 2004. The holocene storegga
5 slide tsunami in the United Kingdom. *Quaternary Science Reviews* **23**, 2291-2321.
- 6 Smith, D. E., Fretwell, P. T., Cullingford, R. A. & Firth, C. R. 2006. Towards improved
7 empirical isobase models of Holocene land uplift for mainland Scotland, UK.
8 *Philosophical Transactions of the Royal Society A: Mathematical, Physical and*
9 *Engineering Sciences* **364**, 949-972.
- 10 Smith, D. E., Cullingford, R. A., Mighall, T. M., Jordan, J. T. & Fretwell, P. T. 2007.
11 Holocene relative sea level changes in a glacio-isostatic area: New data from south-west
12 Scotland, United Kingdom. *Marine Geology* **242**, 5-26.
- 13 Smith, D. E., Stewart, I. S., Harrison, S. & Firth, C. R. 2009. Late Quaternary neotectonics
14 and mass movement in South East Raasay, Inner Hebrides, Scotland. *Proceedings of the*
15 *Geologists' Association* **120**, 145-154.
- 16 Smith, D. E., Davies, M. H., Brooks, C. L., Mighall, T. M., Dawson, S., Rea, B. R., Jordan, J.
17 T. & Holloway, L. K. 2010. Holocene relative sea levels and related prehistoric activity
18 in the Forth lowland, Scotland, United Kingdom. *Quaternary Science Reviews* **29**, 2382-
19 2410.
- 20 Smith, D. E., Hunt, N., Firth, C. R., Jordan, J. T., Fretwell, P. T., Harman, M., Murdy, J.,
21 Orford, J. D. & Burnside, N. G. 2012. Patterns of Holocene relative sea level change in
22 the North of Britain and Ireland. *Quaternary Science Reviews* **54**, 58-76.
- 23 Soudarin, L., Crétaux, J. F. & Cazenave, A. 1999. Vertical crustal motions from the DORIS
24 Space-Geodesy System. *Geophysical Research Letters* **26**, 1207-1210.

- 1 Sowter, A., Bateson, L., Strange, P., Ambrose, K. & Syafiudin, M. F. 2013. DInSAR
2 estimation of land motion using intermittent coherence with application to the South
3 Derbyshire and Leicestershire coalfields. *Remote Sensing Letters* **4**, 979-987.
- 4 Steffen, H. & Wu, P. 2011. Glacial isostatic adjustment in Fennoscandia—a review of data
5 and modeling. *Journal of Geodynamics* **52**, 169-204.
- 6 Stewart, I. S., Firth, C. R., Rust, D. J., Collins, P. E. F. & Firth, J. A. 2001. Recent fault
7 movement and palaeoseismicity in western Scotland: A reappraisal of the Kinloch
8 Hourn fault, Kintail. *Journal of Seismology* **5**, 307-328.
- 9 Stockamp, J., Li, Z., Bishop, P., Hansom, J., Rennie, A., Petrie, E., Tanaka, A., Bingley, R. &
10 Hansen, D. 2015. Investigating Glacial Isostatic Adjustment in Scotland with InSAR
11 and GPS Observations. *Proceedings Fringe 2015 Workshop, Frascati, Italy*. European
12 Space Agency (Special Publication) ESA SP-731.
- 13 Tamisiea, M. E., Mitrovica, J. X. & Davis, J. L. 2007. GRACE gravity data constrain ancient
14 ice geometries and continental dynamics over Laurentia. *Science* **316**, 881-883.
- 15 Teferle, F. N., Bingley, R. M., Dodson, A. H. & Baker, T. F. 2002. Application of the dual-
16 CGPS concept to monitoring vertical land movements at tide gauges. *Physics and*
17 *Chemistry of the Earth* **27**, 1401-1406.
- 18 Teferle, F. N., Bingley, R. M., Williams, S. D. P., Baker, T. F. & Dodson, A. H. 2006. Using
19 continuous GPS and absolute gravity to separate vertical land movements and changes
20 in sea-level at tide-gauges in the UK. *Philosophical Transactions of the Royal Society*
21 *A: Mathematical, Physical and Engineering Sciences* **364**, 917-930.
- 22 Teferle, F. N., Bingley, R. M., Waugh, A. I., Dodson, A. H., Williams, S. D. P. & Baker, T.
23 F. 2007. Sea level in the British Isles: combining absolute gravimetry and continuous
24 GPS to infer vertical land movements at tide gauges. In Tregoning, P., Rizos, C. (eds)
25 *Dynamic Planet*, 23-30. Springer.

- 1 Teferle, F. N., Williams, S. D. P., Kierulf, H. P., Bingley, R. M. & Plag, H. P. 2008. A
2 continuous GPS coordinate time series analysis strategy for high-accuracy vertical land
3 movements. *Physics and Chemistry of the Earth* **33**, 205-216.
- 4 Teferle, F. N., Bingley, R. M., Orliac, E. J., Williams, S. D. P., Woodworth, P. L.,
5 McLaughlin, D., Baker, T. F., Shennan, I., Milne, G. A. & Bradley, S. L. 2009. Crustal
6 motions in Great Britain: evidence from continuous GPS, absolute gravity and Holocene
7 sea level data. *Geophysical Journal International* **178**, 23-46.
- 8 Tong, X., Sandwell, D. T. & Smith-Konter, B. 2013. High-resolution interseismic velocity
9 data along the San Andreas fault from GPS and InSAR. *Journal of Geophysical*
10 *Research: Solid Earth* **118**, 369-389.
- 11 Tooley, M. J. 1974a. Sea-level changes during the last 9000 years in north-west England.
12 *Geographical Journal* **140**, 18-42.
- 13 Tooley, M. J. 1974b. The UNESCO-IGCP Project on Holocene sea-level changes. *The*
14 *International Journal of Nautical Archaeology and Underwater Exploration* **7**, 71-87.
- 15 Tooley, M. J. 1978. Interpretation of Holocene sea-level changes. *Geologiska Föreningens i*
16 *Stockholm Förhandlingar* **100**, 203-212.
- 17 Tooley, M. J. 1982a. Introduction. *Proceedings of the Geologists' Association* **93**, 3-6.
- 18 Tooley, M. J. 1982b. Sea-level changes in northern England. *Proceedings of the Geologists'*
19 *Association* **93**, 43-51.
- 20 Tosi, L., Carbognin, L., Teatini, P., Strozzi, T. & Wegmüller, U. 2002. Evidence of the
21 present relative land stability of Venice, Italy, from land, sea, and space observations.
22 *Geophysical Research Letters* **29**, 3-1-3-4.
- 23 Tushingham, A. M. & Peltier, W. R. 1991. ICE-3G - A new global model of late Pleistocene
24 deglaciation based upon geophysical predictions of post-glacial relative sea level
25 change. *Journal of Geophysical Research* **96**, 4497-4523.

- 1 Van de Plassche, O. 1982. *Sea Level Research – a manual for the collection and evaluation*
2 *of data*. A contribution to IGCP projects 61 and 200. Norwich, UK: Geo Books.
- 3 Wang, H. & Wright, T. J. 2012. Satellite geodetic imaging reveals internal deformation of
4 western Tibet. *Geophysical Research Letters* **39**.
- 5 Wang, T., Perissin, D., Liao, M. & Rocca, F. 2008. Deformation monitoring by long term D-
6 InSAR analysis in Three Gorges area, China. *IEEE International Geoscience and*
7 *Remote Sensing Symposium, IGARSS 2008*, IV-5-IV-8.
- 8 Wdowinski, S., Bock, Y., Zhang, J., Fang, P. & Genrich, J. 1997. Southern California
9 permanent GPS geodetic array: spatial filtering of daily positions for estimating
10 coseismic and postseismic displacements induced by the 1992 Landers earthquake.
11 *Journal of Geophysical Research-Part B-Solid Earth-Printed Edition* **102**, 18057-
12 18070.
- 13 Wei, M., Sandwell, D. & Smith-Konter, B. 2010. Optimal combination of InSAR and GPS
14 for measuring interseismic crustal deformation. *Advances in Space Research* **46**, 236-
15 249.
- 16 Williams, S. D. P., Baker, T. F. & Jeffries, G. 2001. Absolute gravity measurements at UK
17 tide gauges. *Geophysical Research Letters* **28**, 2317-2320.
- 18 Woodroffe, S. A. & Barlow, N. L. M. 2015. Reference water level and tidal datum. *In*
19 Shennan, I., Long, A. J. & Horton, B. P. (eds) *Handbook of Sea-Level Research*.
20 Chichester, UK: John Wiley & Sons, Ltd.
- 21 Woodworth, P. L., Tsimplis, M. N., Flather, R. A. & Shennan, I. 1999. A review of the trends
22 observed in British Isles mean sea level data measured by tide gauges. *Geophysical*
23 *Journal International* **136**, 651-670.
- 24 Woodworth, P. L., Teferle, F. N., Bingley, R. M., Shennan, I. & Williams, S. D. P. 2009.
25 Trends in UK mean sea level revisited. *Geophysical Journal International* **176**, 19-30.

- 1 Wöppelmann, G., Zerbini, S. & Marcos, M. 2006. Tide gauges and Geodesy: a secular
2 synergy illustrated by three present-day case studies. *Comptes Rendus Geoscience* **338**,
3 980-991.
- 4 Wright, T. J., Parsons, B. & Fielding, E. 2001. Measurement of interseismic strain
5 accumulation across the North Anatolian Fault by satellite radar interferometry.
6 *Geophysical Research Letters* **28**, 2117-2120.
- 7 Wright, T. J., Lu, Z. & Wicks, C. 2003. Source model for the Mw 6.7, 23 October 2002,
8 Nenana Mountain Earthquake (Alaska) from InSAR. *Geophysical Research Letters* **30**.
- 9 Wright, T. J., Parsons, B., England, P. C. & Fielding, E. J. 2004a. InSAR observations of low
10 slip rates on the major faults of western Tibet. *Science* **305**, 236-239.
- 11 Wright, T. J., Parsons, B. E. & Lu, Z. 2004b. Toward mapping surface deformation in three
12 dimensions using InSAR. *Geophysical Research Letters* **31**.
- 13 Zhang, L., Ding, X., Lu, Z., Jung, H.-S., Hu, J. & Feng, G. 2014. A novel multitemporal
14 InSAR model for joint estimation of deformation rates and orbital errors. *IEEE*
15 *Transactions on Geoscience and Remote Sensing* **52**, 3529-3540.

Figure captions

Definition of Sea Level (SL), Relative Sea Level change (RSL) and Vertical Land Motion (VLM) at location (z) and times (t) and (t_0):

$$SL(z,t) = G(z,t) - R(z,t)$$

$$\Delta G(z,t) = G(z,t) - G(z,t_0)$$

$$\Delta R(z,t) = R(z,t) - R(z,t_0) = \text{VLM}$$

$$\text{RSL}(z,t) = SL(z,t) - SL(z,t_0)$$

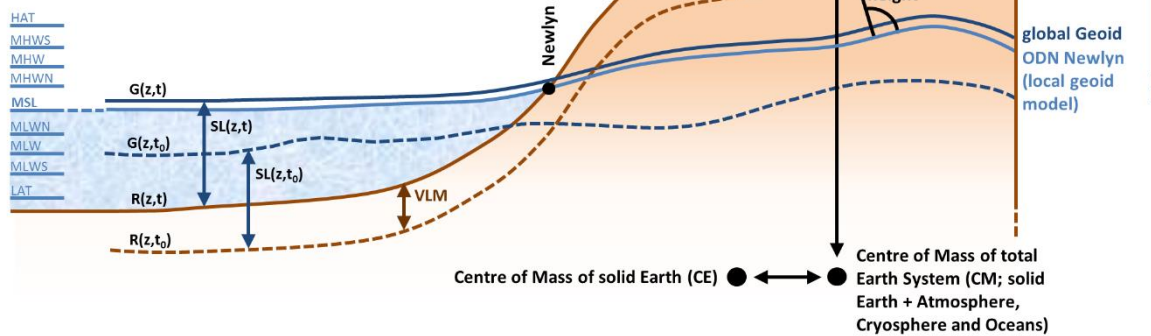


Figure 1 Schematic overview of reference surfaces used when measuring and modelling RSL change and vertical land motion (VLM) of the British Isles (after Shennan *et al.* 2012, extended). Sea level (SL) at time t and location z is defined as the distance between Geoid (G) and solid Earth surface (R), which both relate to the centre of the Earth. G is the long-term averaged mean sea surface over several decades (Shennan *et al.* 2012). Around Great Britain, the global Geoid lies about 80 cm above a local geoid model (Ordnance Datum Newlyn – ODN) due to sea surface topography. ODN is defined by Mean Sea Level measured at Newlyn tide gauge between 1915 and 1921. Orthometric height of a point A is height above ODN (Ordnance Survey 2015). Eustatic Sea Level change and isostatic changes to the gravitational field can cause change in G between a time t and a reference time t_0 . VLM is the change in solid Earth surface R between a time t and t_0 . RSL change refers to the difference in Sea Level (SL) at a time t relative to t_0 . Variations in water levels from MSL are indicated on the left hand side for a semidiurnal tidal system (for definitions see main text and Woodroffe & Barlow 2015; Shennan 2015). MHWS and HAT are a common reference

1 of sea level index points or isobase models of RSL change. ITRF is the International
2 Terrestrial Reference Frame mostly used for GPS referencing (ITRF2008 is the latest one),
3 relative to the CM of the total Earth System. CE is used in GIA modelling.



5
6 **Figure 2** Staircases of emerged gravel ridges uplifted by glacial isostatic adjustment at Shian
7 Bay, Isle of Jura. The highest ridge is about 35m ASL (see Castillo *et al.* 2013). In the right
8 foreground is a glacially striated *roche moutonnée*.



Figure 3 Isolation basin in northwestern Scotland, separated from the influences of the sea and its highest tides.

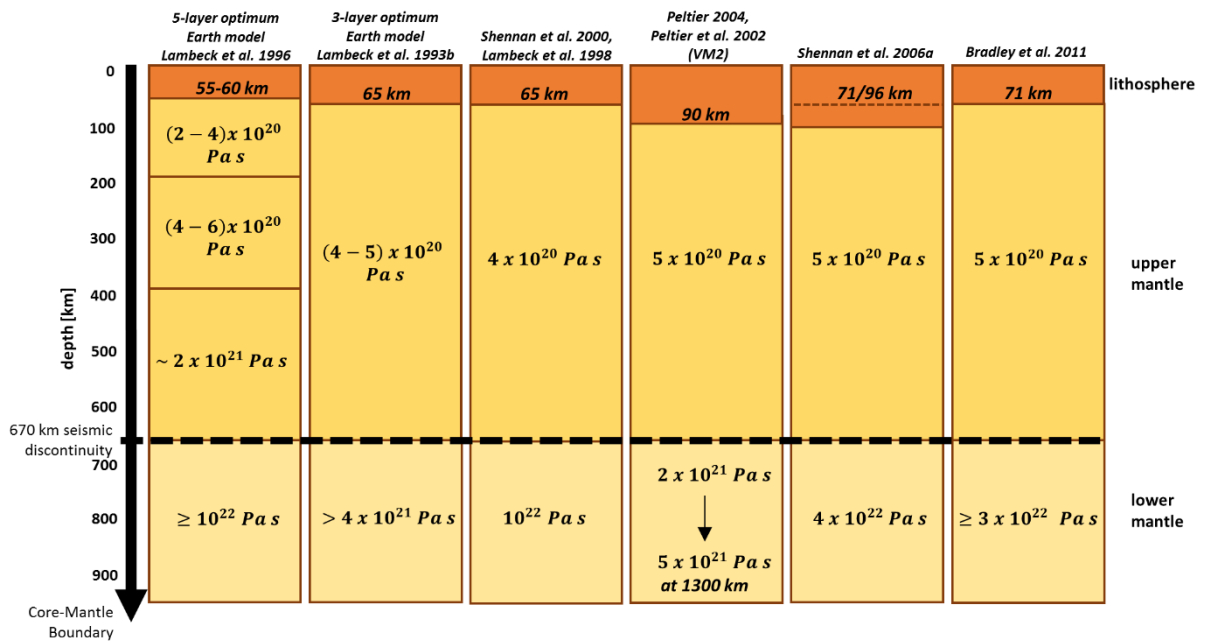
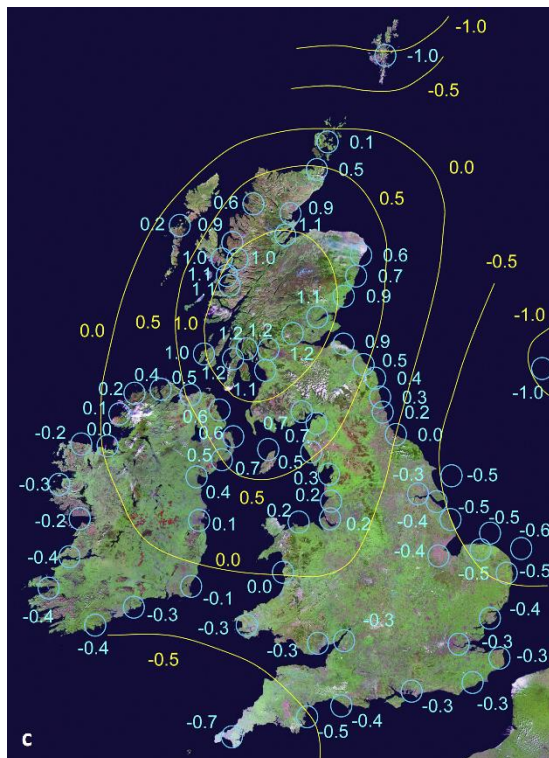
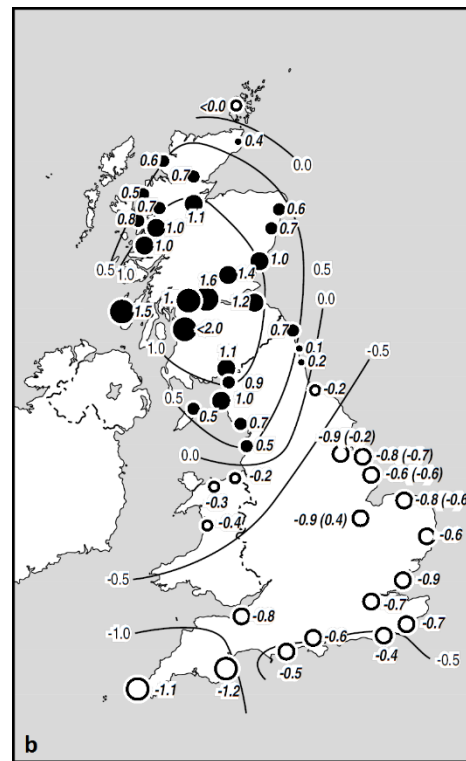
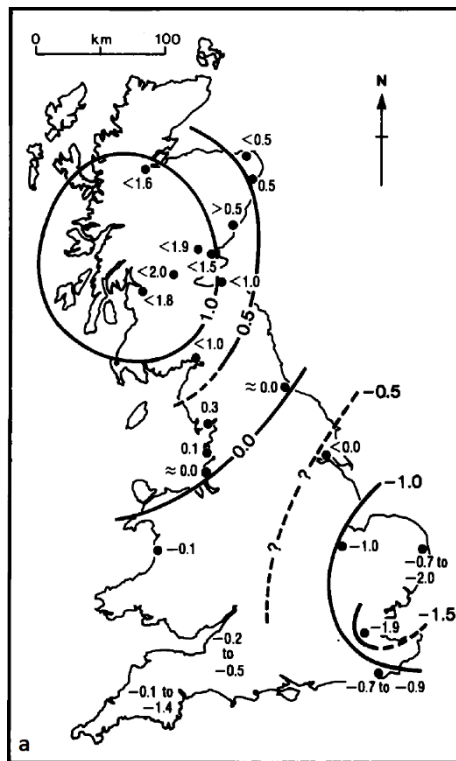


Figure 4 Earth-model configurations in GIA studies mentioned in this paper



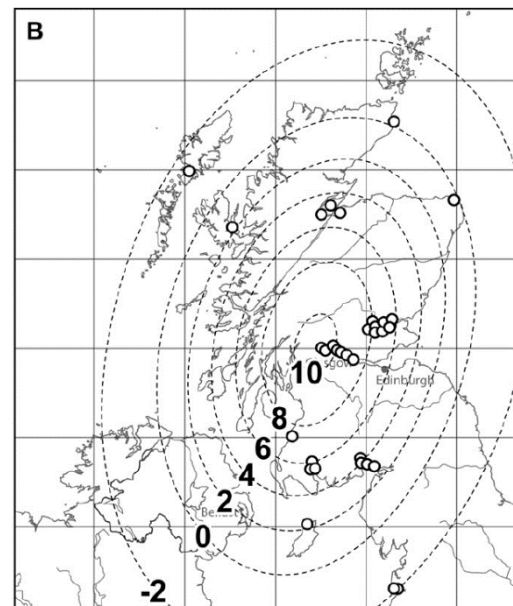
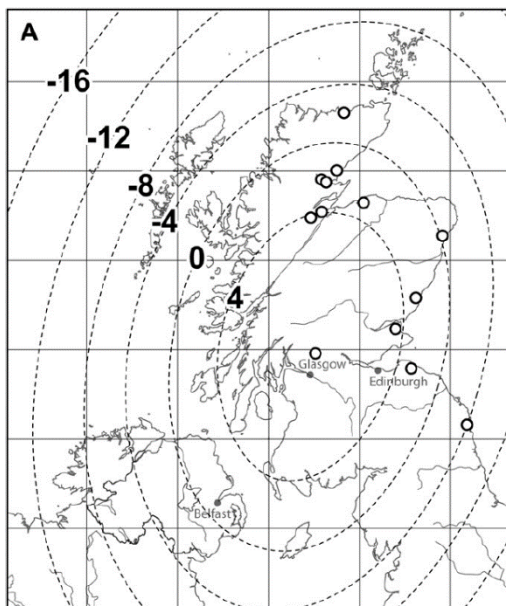
1 **Figure 5** Evolution of patterns of Late Holocene glacial isostatic adjustment in mm yr^{-1} for
2 the British Isles, modelled using geological sea-level reconstructions: (a) crustal movements,
3 constrained with data since 8800 BP; (b) relative land-/ sea-level changes from data since
4 4000 cal. yr BP; (c) relative land-/ sea-level changes from data since 1000 BP, with a centre

of relative land uplift (positive values) over northern Scotland and three sub-centres of relative subsidence (negative values) over southwest England, the southern North Sea and the Shetland Isles.

(a) Copyright (1989) Wiley. Used with permission from Shennan, I., Holocene crustal movements and sea-level changes in Great Britain, *Journal of Quaternary Science*, John Wiley & Sons.

(b) Copyright (2002) Wiley. Used with permission from Shennan, I. & Horton, B., Holocene land- and sea-level changes in Great Britain, *Journal of Quaternary Science*, John Wiley & Sons.

(c) Copyright (2012) Wiley. Used with permission from Shennan, I., Milne, G. & Bradley, S. L., Late Holocene vertical land motion and relative sea-level changes: lessons from the British Isles, *Journal of Quaternary Science*, John Wiley & Sons.



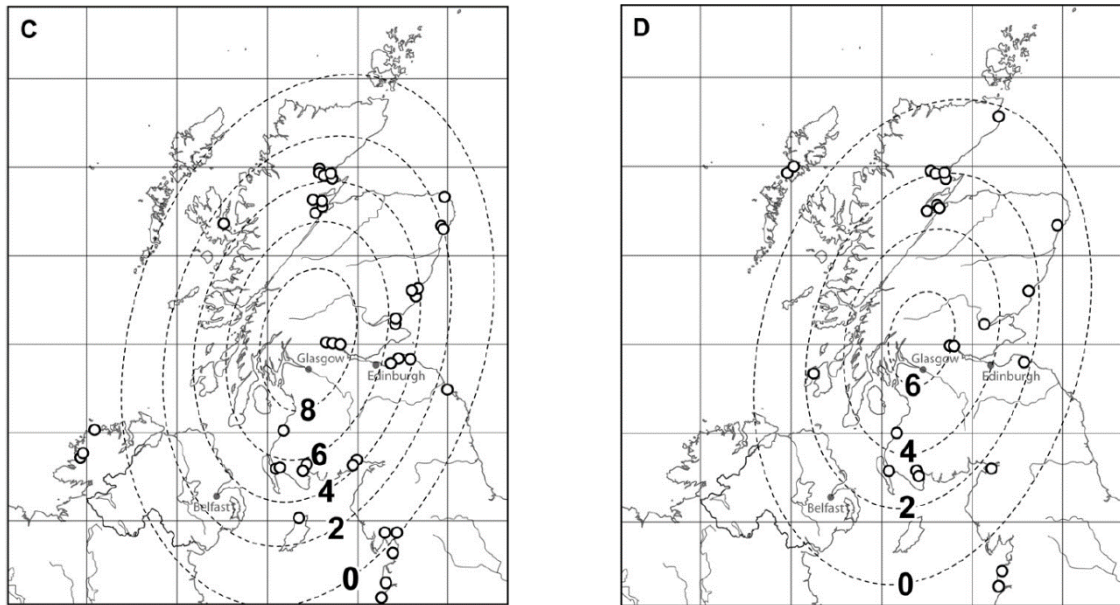


Figure 6 Spatial pattern of RSL change during the Holocene as indicated by the Storegga (A), Main Postglacial (B), Blairdrummond (C) and Wigtown (D) Shorelines (chronologically ordered) based on Gaussian Quadratic Trend Surface modelling and constrained to a common axis and centre in the South-East Grampian Highlands of Scotland. Displayed are heights above MHWS with location of altitudinal data points (circles). The greater the distance from the centre of uplift in central Scotland, the more visible the younger shorelines become on the surface.

Reprinted from Quaternary Science Reviews, 54, Smith, D. E., Hunt, N., Firth, C. R., Jordan, J. T., Fretwell, P. T., Harman, M., Murdy, J., Orford, J. D. & Burnside, N. G., Patterns of Holocene relative sea level change in the North of Britain and Ireland, 58-76, Copyright (2012), with permission from Elsevier.

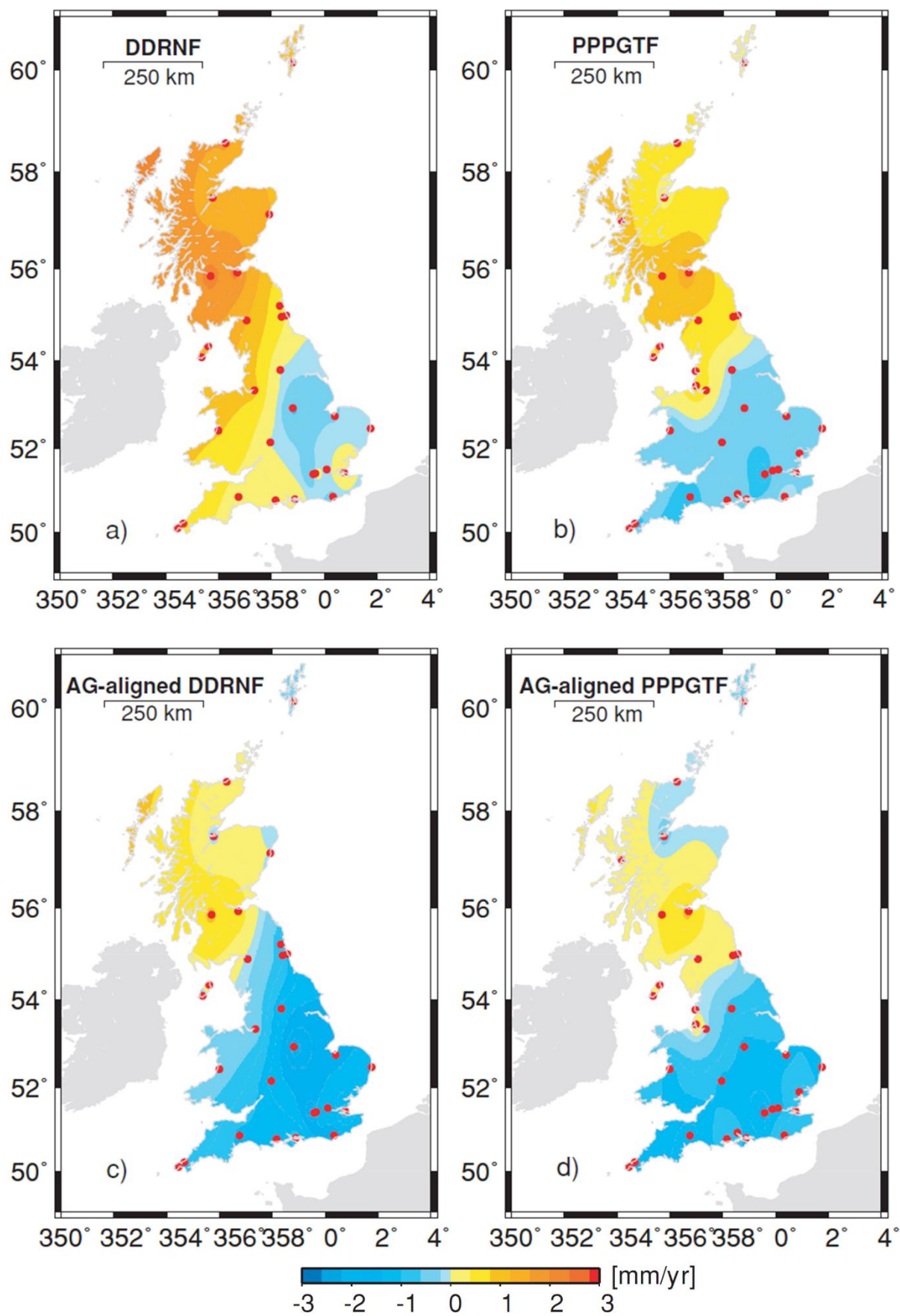


Figure 7 Vertical crustal motions in Great Britain from CGPS (a, b) and AG-aligned CGPS (c, d) estimates for two CGPS processing techniques: DDRNF denotes a series of daily double-difference (DD) regional network (RN) solutions, while PPPGTF stands for a series of daily precise point positioning (PPP) globally transformed (GT) solutions. Processing time frame: 1997-2005. F means spatial filtering. Red dots represent CGPS stations.

Teferle, F. N., Bingley, R. M., Orliac, E. J., Williams, S. D. P., Woodworth, P. L., McLaughlin, D., Baker, T. F., Shennan, I., Milne, G. A. & Bradley, S. L., Crustal motions in Great Britain: evidence from continuous GPS, absolute gravity and Holocene sea level data, *Geophysical Journal International*, 2009, 178, 1,23-46, by permission of Oxford University Press, published on behalf of the Royal Astronomical Society.

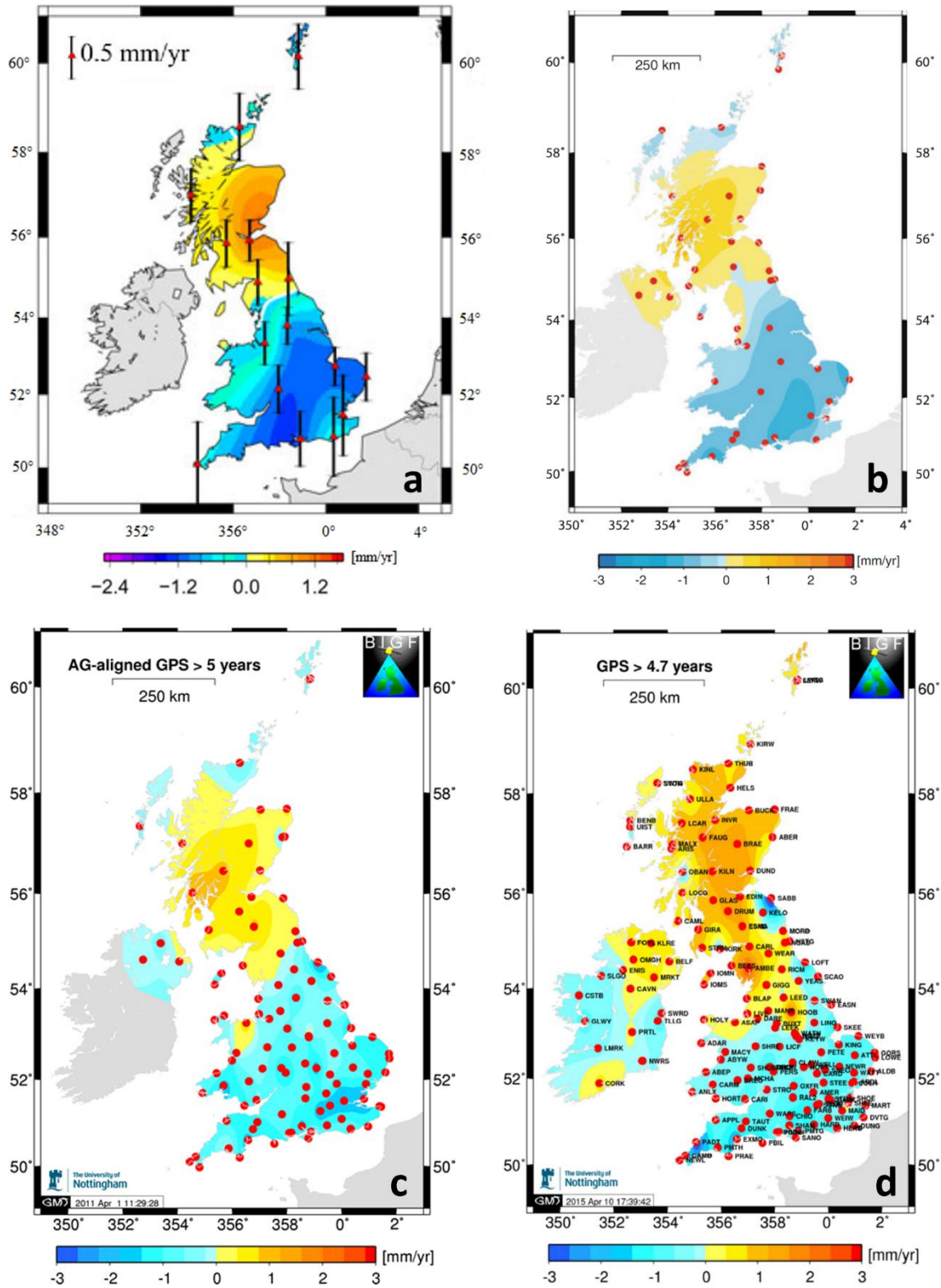


Figure 8 Comparison of maps of vertical land motion derived from AG-aligned CGPS station measurements in Great Britain and Ireland (stations indicated by red dots). They differ in processing time-frame, amount of included CGPS receivers, reference frame implementation and minimum time-series duration: (a) processing time frame 1997–2005, 16

CGPS sites, motion calculated relative to station in Sheerness, > 4 years minimum time-series duration; (b) 1997-2008, 46 CGPS sites, semi-global reference frame implementation with 37 IGS stations within ITRF2005, > 6 years minimum time-series duration; (c) 1997-2010, 104 CGPS sites, global reference frame network within ITRF2008, > 5 years; (d) 1997-2015, 158 CGPS sites, global reference frame implementation, IGB08, > 4.7 years.

(a) Bradley, S. L., Milne, G. A., Teferle, F. N., Bingley, R. M. & Orliac, E. J., Glacial isostatic adjustment of the British Isles: new constraints from GPS measurements of crustal motion, *Geophysical Journal International*, 2009, 178, 14-22, by permission of Oxford University Press, published on behalf of the Royal Astronomical Society.

(b) *Geodesy for Planet Earth 2012*, 665-671, New estimates of recent-day crustal/land motions in the British Isles based on the BIGF network, Hansen, D. N., Teferle, F. N., Bingley, R. M. & Williams, S. D. P., Figure 82.5b, with permission from Springer Science + Business Media.

(c) published in Greaves *et al.* (2013), reused with permission from BIGF.

(d) published in Greaves *et al.* (2015), reused with permission from BIGF.

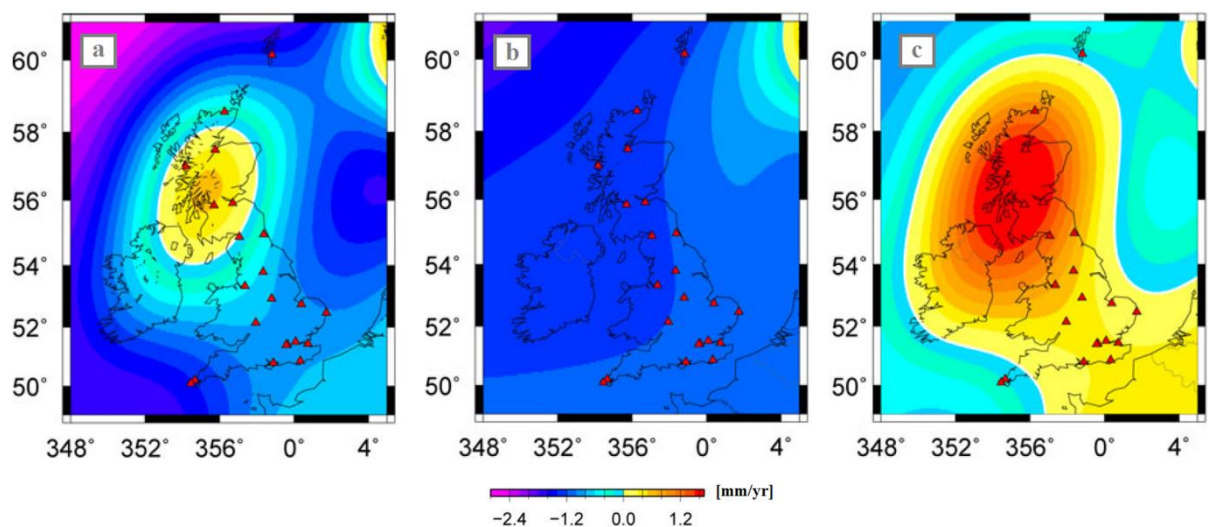


Figure 9 Modelled current rates of land uplift (5 km x 5 km grid) from model constrained by both geological sea-level observations and AG-aligned CGPS estimates (a). (b) and (c) decomposed total signal of (a), with (b) showing the effects of non-local ice sheets and (c) showing effects of British-Irish ice sheet and ocean loading only.

Bradley, S. L., Milne, G. A., Teferle, F. N., Bingley, R. M. & Orliac, E. J., Glacial isostatic adjustment of the British Isles: new constraints from GPS measurements of crustal motion, *Geophysical Journal International*, 2009, 178, 14-22, by permission of Oxford University Press, published on behalf of the Royal Astronomical Society.

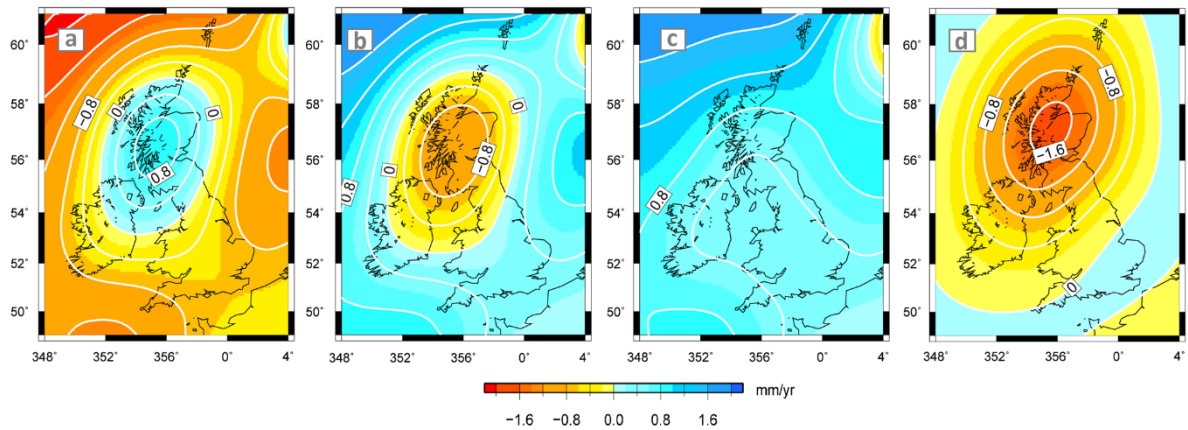


Figure 10 Modelled present-day vertical land motion (a) and relative sea-level change (b) with (c) and (d) showing the decomposed total sea-level signal from (b) (c: from far-field ice sheets, d: from British–Irish ice sheet only).

Copyright (2011) Wiley. Used with permission from Bradley, S. L., Milne, G. A., Shennan, I. & Edwards, R. J., An improved glacial isostatic adjustment model for the British Isles, *Journal of Quaternary Science*, John Wiley & Sons.

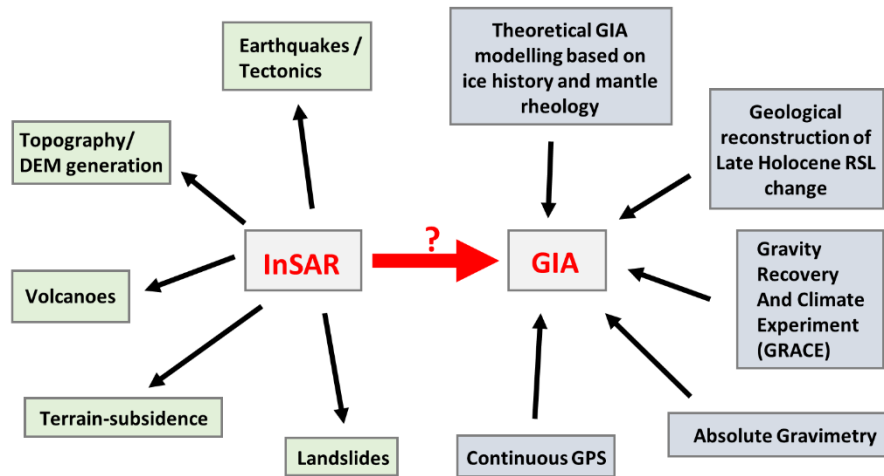


Figure 11 Interface between InSAR and GIA: Research areas, where InSAR is commonly used as a tool (left) vs. research methods that are usually applied to analyse GIA (right). Research studying the application of InSAR to measure GIA-induced VLM directly has been scarce.

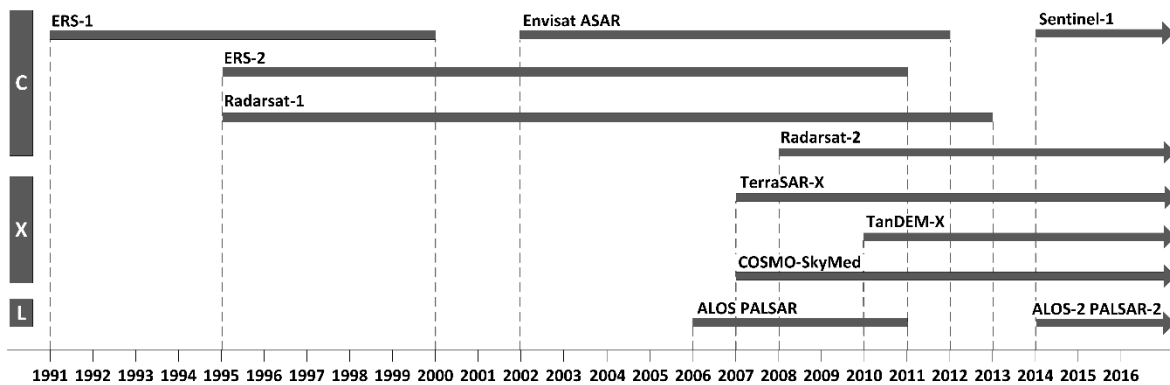


Figure 12 Temporal coverage of available SAR sensors and their frequency bands.